THE PHOSPHODIESTERASE-4 INHIBITOR ROFLUMILAST REVERTS PROTEOLYSIS IN SKELETAL MUSCLE CELLS OF PATIENTS WITH COPD CACHEXIA

Esther Barreiro[1,2], Ester Puig-Vilanova[1], Anna Salazar-Degracia[1], Sergi Pascual-Guardia[1], Carme Casadevall[1,2], Joaquim Gea[1,2]

[1]Pulmonology Department-Muscle and Respiratory System Research Unit (URMAR), IMIM-*Hospital del Mar*, *Parc de Salut Mar*, Health and Experimental Sciences Department (CEXS), *Universitat Pompeu Fabra* (UPF), Barcelona Biomedical Research Park (PRBB), C/ Dr. Aiguader, 88, Barcelona, E-08003 Spain.

[2]*Centro de Investigación en Red de Enfermedades Respiratorias* (CIBERES), *Instituto de Salud Carlos* III (ISCIII), C/ Monforte de Lemos 5, Madrid, E-28029 Spain.

Corresponding author: Dr. Esther Barreiro, Pulmonology Department-URMAR, IMIM-Hospital del Mar, PRBB, C/ Dr. Aiguader, 88, Barcelona, E-08003 Spain, Telephone: (+34) 93 316 0385, Fax: (+34) 93 316 0410, e-mail: ebarreiro@imim.es.

Running title: Roflumilast effects in COPD cachectic myotubes

Word count: 5,652

ABSTRACT

Peripheral muscle weakness and mass loss are characteristic features in severe COPD. We hypothesized that the phosphodiesterase-4 inhibitor roflumilast-induced cAMP may ameliorate proteolysis and metabolism in skeletal muscles of COPD patients with severe muscle wasting. In myogenic precursor cells (isolated from muscle biopsies and cultured up to obtain differentiated myotubes) from 10 severe COPD patients and 10 healthy controls, which were treated with 1 microM roflumilast N-oxide (RNO) for three time-cohorts (1h, 6h, and 24h), genes of antioxidant defense and oxidative stress marker, myogenesis and muscle metabolism, proteolysis (tyrosine release assay) and ubiquitin-proteasome system markers, autophagy, and myosin isoforms were analyzed using RT-PCR and immunoblotting. In COPD patients, at 6h-RNO treatment, myotube tyrosine release, total protein ubiquitination, and *TRIM32* levels were significantly lower than healthy controls, whereas at 24h-RNO treatment, myotube *MyHC*-I and *MyHC*-IIx expression levels were upregulated in both patients and controls. In the 6h-RNO cohort, in patients and controls, myotube expression of *NRF*2 and its downstream antioxidants, *Sirtuin-1*, *FN*14, and *IGF*-I was upregulated, while that of *MEF*2C, *MYOD*, *Myogenin*, *Myostatin*, *Atrogin*-1, and *MuRF*-1 was downregulated. In myotubes of severe COPD patients with cachexia, roflumilast-induced cAMP signaling exerts beneficial effects by targeting muscle protein breakdown (tyrosine release) along with reduced expression of proteolytic markers of the ubiquitin-proteasome system and that of myostatin. In both patients and controls, roflumilast also favored antioxidant defense through upregulation of *NRF*2 pathway and that of the histone deacetylase Sirtuin-1, while it improved the expression of slow- and fast-twitch myosin isoforms. These findings show that muscle dysfunction and wasting may be targeted by roflumilast-induced cAMP signaling in COPD. These results have potential therapeutic implications as this PDE4 inhibitor is currently available for the treatment of systemic inflammation and exacerbations in patients with severe COPD. **Word count:** 289

KEY WORDS: COPD-induced muscle wasting; myotubes; roflumilast; antioxidant defense; proteolysis; myosin heavy chain

NEW & NOTEWORTHY

In myotubes of cachectic COPD patients, c-AMP signaling exerted beneficial effects by targeting muscle proteolysis and reducing gene expression of proteolytic markers of ubiquitin-proteasome system and that of Myostatin. In myotubes of patients and controls, roflumilast also favored antioxidant defense through upregulation of NRF2 pathway, that of Sirtuin-1, and upregulated gene expression of slow- and fast-twitch isoforms. These findings have potential clinical implications for the treatment of muscle wasting in patients with COPD and cachexia.

Word count: 75

Abbreviations: COPD, Chronic obstructive pulmonary disease; CREB, cAMP response element-binding; PDE, phosphodiesterase; cAMP, cyclic adenosine monophosphate; GOLD, Global Initiative for COPD; FoxO, forkhead box O; BMI, body mass index; FFMI, fat-free mass index; QMVC, maximum voluntary contraction; VL, vastus lateralis; DMEM, Dulbecco’s modified Eagle's medium; PM, proliferation medium; FBS, fetal bovine serum; PSF, penicillin/streptomicin/fungizone-solution; bFGF, basic fibroblast growth factor; EGF, epidermal growth factor; PBS, phosphate-buffered saline; HS, horse serum; DMSO, dimethyl sulfoxide; RNO, roflumilast N-oxide; RNA, ribonucleic acid; qRT-PCR, quantitative real time-PCR amplification; MGB, taqMan-minor groove binder; FAM, fluorescein amidite; qPCR, real-time polymerase chain reaction; GAPDH, glyceraldehyde-3-phosphate dehydrogenase; mRNA, messenger RNA; HEPES, 2-hydroxyethyl)-1-piperazineethanesulfonic acid; EDTA, ethylenediaminetetraacetic acid; PMSF, phenylmethylsulfonyl fluoride; BSA, bovine serum albumin; PVDF, polyvinylidene difluoride; MDA, malondialdehyde; HRP, horseradish peroxidase; BKH, Krebs-HEPES buffer; NADPH, NOX, nicotinamide adenine dinucleotide phosphate; NRF2, nuclear factor

77 (erythroid-derived 2)-like 2; NQO, NADPH dehydrogenase quinone; HO-1, heme oxygenase;
78 GCLC, glutamate-cysteine ligase catalytic; GCLM, GCL modifier; IGF1, insulin-like growth
79 factor; TFAM, mitochondrial transcription factor A; MEF, myocyte-specific enhancer factor;
80 MYOD, myogenic differentiation; PGC, peroxisome proliferator-activated receptor-gamma
81 coactivator; FN, fibroblast growth factor inducible; FNDC, fibronectin type III domain-
82 containing protein; MuRF, muscle RING-finger protein; PKA, protein kinase A; TRIM,
83 tripartite motif-containing protein; LC, microtubule-associated protein 1A/1B-light chain;
84 MyHC, myosin heavy chain; DNA, deoxyribonucleic acid.
85

INTRODUCTION

Chronic obstructive pulmonary disease (COPD) is a highly prevalent condition, which represents a major cause of mortality worldwide (35; 36; 55). Patients with COPD usually have systemic manifestations that involve reduced physical activity and exercise capacity, nutritional abnormalities, weakness of muscles of the lower limbs along with muscle mass loss (2; 3; 32; 34-36; 50; 55). Importantly, all these systemic manifestations of COPD are reliable predictors of mortality independently of the severity of the airways obstruction (2; 3; 32).

In the multifactorial etiology of COPD skeletal muscle weakness, factors such as cigarette smoking, hypoxia and hypercapnia, frequent exacerbations, and deconditioning are counted among the most relevant players (3; 32). Moreover, several biological mechanisms have also been demonstrated to underlie skeletal muscle dysfunction and mass loss in patients with COPD such as structural abnormalities, reduced oxidative metabolism and other metabolic disruptions, epigenetic alterations, and increased oxidative stress, proteolytic activity and autophagy (2; 3; 32; 39-42). Despite the progress achieved in understanding the etiology and underlying biology of COPD muscle dysfunction, implementation of therapeutic strategies specifically targeted to alleviate muscle weakness and mass loss in these patients is still at its infancy.

Roflumilast is a potent selective inhibitor of the enzyme phosphodiesterase-4 (PDE4) used in clinical settings that leads to increased levels of cyclic adenosine monophosphate (cAMP) in cells. The rise in cAMP exerts anti-inflammatory actions by targeting immune cells, which has been shown to benefit lung function in patients with moderate-to-severe COPD (7; 43). Furthermore, roflumilast has been recently demonstrated to modify the shift from the frequent to the more infrequent exacerbator state in patients with severe COPD as classified by the Global Initiative for COPD (GOLD) strategy (55).

On the other hand, most of the effects of roflumilast may be attributed to the actions

of the well-characterized signaling molecule cAMP. In skeletal muscles, acute cAMP signaling has been shown to regulate several key processes such as contractility and both calcium and glycogen metabolism, which translate into increased force generation and a faster recovery of ion balance during prolonged contractions as in exercise (5). Increased production of cAMP leads to activation of protein kinase A (PKA), which has been associated with the inhibition of proteolytic pathways along with increased protein synthesis (48). Muscle proteolysis can be blocked through inhibition of either calcium-dependent proteolysis or adenosine triphosphate (ATP)-dependent proteolysis cellular processes (48). Importantly, cAMP/PKA signaling promotes protein synthesis as a result of the initiation of protein transcription (48). PKA may diffuse passively into the nucleus thus regulating the expression of target genes via phosphorylation of cAMP response element-binding (CREB) (31). Specifically, improvements in muscle function and atrophy were seen in animal models of disuse, denervation, aging, and muscular dystrophy in response to cAMP signaling induced by pharmacological agents (5). In cultured myotubes obtained from rat skeletal muscles, treatment with the phosphodiesterase inhibitor isobutylmethylxanthine increased cAMP levels which induced a reduction in ubiquitin-proteasome activity and in the expression of markers of this proteolytic pathway (23). Transcription factors involved in muscle mass loss and atrophy such as forkhead box O (FoxO)3 were also inactivated by the isobutylmethylxanthine-induced accumulation of cAMP in the rat cultured myotubes (23). Whether increased cAMP may improve metabolism and proteolysis in atrophying myotubes of patients with COPD remains an open question.

On this basis, we hypothesized that roflumilast-induced cAMP signaling increased levels may ameliorate proteolysis and metabolism in skeletal muscles of COPD patients with severe muscle wasting. The present investigation was conducted in cultured myotubes directly obtained from cachectic COPD patients. This experimental approach enabled us to control for the potential systemic effects induced by roflumilast in organs other than skeletal muscles.

Moreover, the potential contribution of factors associated with the muscle niche (environment) characteristic of in vivo models was avoided in the cultured myotubes. Accordingly, our objectives were as follows: 1) to assess levels of markers of the ubiquitin-proteasome system and proteolysis (tyrosine release) and 2) to determine markers and transcription factors involved in muscle metabolism and regeneration in response to treatment with roflumilast (similar to the dose administered in patients) of human primary cultured myotubes at different time-points (to explore short-, medium-, and long-term effects of roflumilast). Myotubes from biopsies of healthy control subjects were also studied.

METHODS

Study subjects

Ten patients with severe COPD according to currently available guidelines (35; 36; 55) and altered body composition (muscle wasting and cachexia) together with 10 age-matched sedentary controls with normal respiratory function were enrolled in a cross-sectional study from the COPD Clinic at *Hospital del Mar* (Barcelona). Muscle wasting was defined as a body mass index (BMI) $\leq$ 21 kg/m^2 and a fat-free mass index (FFMI) $\leq$ 18 kg/m^2, cut-off value established for a Mediterranean population in accordance with both previously published criteria (18; 41; 42) and the international consensus on the definition of cachexia (16; 17). Control subjects were non-smokers (50% ex-smokers and 50% never-smokers) sedentary control subjects recruited from the general population (patient's relatives or friends) at Hospital del Mar, while patients were active smokers or ex-smokers (40% and 60%, respectively). All patients were on inhaled bronchodilators. They were clinically stable at the time of the study entry, without episodes of exacerbation or oral steroid treatment in the previous four months. None of them presented significant comorbidities. Both patients and healthy controls were Caucasian.

Exclusion criteria. Exclusion criteria for COPD patients and control subjects included the

presence of other chronic respiratory or cardiovascular disorders, acute exacerbations in the last 3 months, limiting osteoarticular condition, chronic metabolic diseases, suspected para-neoplastic or myopathic syndromes, and/or treatment with drugs known to alter muscle structure and/or function including systemic corticosteroids. COPD patients and healthy controls were qualified as sedentary after being specifically inquired about whether they were conducting any regular outdoor physical activity, going regularly to the gymnasium, or participating in any specific training program. Specifically, sedentarism was defined on the basis of the following criteria: 1) if subjects were not engaged in one or more of these activities: walking, running, bike riding, swimming, dancing, gardening, or weight lifting more than five times per week, 2) not performing at least 3 hours/week of endurance-type physical activity, and/or 3) inactive general state in which leisure time physical activity was minimal (44).

The current cross-sectional investigation was designed in accordance with both the ethical standards on human experimentation in our institutions and the World Medical Association guidelines (Helsinki Declaration of 2008) for research on human beings. Approval was obtained from the institutional Ethics Committee on Human Investigation (project number 2014/5504/I, IMIM-*Hospital del Mar*, Barcelona). Informed written consent was obtained from all individuals.

Anthropometrical and functional assessment

Anthropometrical evaluation included BMI and determination of the FFMI using bioelectrical impedance (41; 42). Nutritional parameters were also evaluated through conventional blood tests. Lung function was evaluated through determination of spirometric values, static lung volumes, diffusion capacity, and blood gases using standard procedures and established reference values (45-47). Exercise capacity was assessed through the measurement of the six-minute walking distance following current guidelines (1; 3).

In both patients and controls, quadriceps muscle strength was evaluated through the determination of isometric maximum voluntary contraction (QMVC) of the dominant lower limb as formerly described (41; 42).

Muscle biopsy and blood samples

With the aim to prevent potentially exhausting physical exercise that could interfere with the results obtained in muscles, all study subjects were recommended to maintain their regular daily physical activity as usually 10-14 days before undergoing the surgical biopsy procedures on outpatient basis. Additionally, patients and healthy subjects rested for one hour on a chair with legs half-flexed, time at which blood samples were obtained, right before initiation of the surgical procedures (19; 41; 42). Specimens from the *vastus lateralis* (VL) portion of the quadriceps muscle were obtained from all subjects using the open biopsy technique as previously described (2; 40-42). Primary myogenic cultures were conducted on the muscle biopsy specimens obtained from both patients and healthy controls.

Blood samples were drawn at 8:00h am after an overnight fasting period in both patients and healthy controls.

Myogenic precursor cell isolation and cultures

Muscle samples were placed on sterile petri dishes in Dulbecco’s modified Eagle's medium (DMEM) and trimmed of connective and fat tissues. Muscle specimens were minced finely and digested in 0.2 % collagenase type I (Sigma-Aldrich, St. Louis, MO, USA) at 37 °C for one hour with occasional agitation. The resulting suspension of particles was further digested with 0.05 % trypsin at 37 °C for 30 minutes. Samples were then filtered through a 100-micrometer cell strainer. Cell suspensions were cultured on 1.5 % gelatin-coated petri-dishes in proliferation medium (PM) consisting of 3:1 mixture of DMEM/Medium-199 and supplemented with the following compounds: 20% fetal bovine serum (FBS), 2 mM L-glutamine, 1% penicillin/streptomicin/fungizone-solution (PSF), 2.5 ng/mL recombinant human basic fibroblast growth factor (bFGF), 10 microgram/mL recombinant human insulin,

and 10 ng/mL recombinant human epidermal growth factor (EGF). All the study experiments described below were performed on muscle cells between passages 4-6 of the primary cultures, time at which the number of cells needed to perform all the experiments was reached and the myotubes still preserved their differentiating features (as seen under light microscopy, fusion of myoblasts to form multinucleated myotubes).

Myogenic purity assessment. Previously published procedures were followed (13).To evaluate the myogenic purity, cell monolayers grown on chamber culture slides were fixed with 1:1 methanol-acetone at -20ºC for 10 minutes before immunocytochemical characterization. Myoblasts were identified using anti-desmin antibody (Thermo Scientific, Waltham, MA, USA). After a 30-minute incubation with the antibody, slides were washed and incubated for 30 minutes with biotinylated universal secondary antibody followed by another 30-minute incubation with horseradish-conjugated streptavidin and diaminobenzidine for 5 minutes (kit LSAB+HRP Dako Cytomation Inc., Carpinteria, CA, USA) as a substrate. Slides were counterstained with hematoxylin for two more minutes, dehydrated and mounted for conventional microscopy. Images were captured under light microscopy (x200, Olympus BX 61, Olympus Corporation, Tokyo, Japan) in 20 randomly selected fields of each muscle specimen. In all samples from both patients and controls more than 94 % desmin positive cells were identified (13) (Figures E1A-1C).

Experimental procedures and groups

For the culture of myotubes, myogenic differentiation was induced by plating cells at a high density (10^4 cells / cm^2) and allowing them to adhere in PM overnight. After a 24-hour period of cell attachment in PM, cells were washed twice in phosphate-buffered saline (PBS) and induced to differentiate over a five-day period in differentiation medium (DMEM/Medium-199, 3:1 mixture) supplemented with 2% horse serum (HS), which contained 2 mM L-glutamine, 100 U/mL penicillin, and 0.1 mg/mL streptomycin in the presence of 0.1% dimethyl sulfoxide (DMSO).

Roflumilast N-oxide (RNO), the active metabolite of roflumilast accounting for > 90% of PDE4 inhibition was provided by the pharmaceutical company Takeda (Chuo-ku, Osaka, Japan) for experimental *in vitro* use only. One hundred mM RNO was dissolved in DMSO at a 10 mM stock solution which was stored at -20ºC. RNO stock solution was sterilized in a MILLEX syringe filter (0.22 microm x 33 mm, Millipore Iberica, Darmstadt, Germany), and was diluted 1:10 in 100% DMSO, resulting in a 1 mM RNO / 100% DMSO solution. Moreover, this solution was further diluted 1:100 in the cell culture medium to obtain the desired final concentration of 1 microM in 0.1% DMSO solution. The final concentration used (1 microM RNO) was the minimum concentration required to inhibit PDE4 activity according to a previous pilot study conducted on human cells (unpublished observations). This concentration (1 microM RNO) was equivalent to dosage used in clinical settings: 500-mg tablets of the active compound roflumilast administered every 24h in COPD patients.

The differentiated myotube sets of cultures were divided into the following groups: 1) baseline group (myotubes in 0.1% DMSO), 2) 24h-RNO group (myotubes treated with 1 microM RNO for 24 hours, 3) 6h-RNO group (myotubes treated with 1 microM RNO for six hours, and 4) 1h-RNO group (myotubes treated with 1 microM RNO for one hour). Graphical representation of these experimental groups is shown in Figure 1. Internal experimental controls consisting of independent sets of myotubes that were only treated with the vehicle (0.1% DMSO) were also conducted. The molecular biology experiments required to fulfill the study objectives were performed in the muscle differentiated cells, while proliferating cells (myoblasts) were used only as internal controls in order to validate the model. Representative images of differentiated cells (myotubes) are shown in Figure 2, together with proliferating cells (myoblasts) to check the differences in phenotype between the two types of cells.

Molecular biology analyses

At the end of either RNO or DMSO treatments, the cultured cells from differentiated cells were immediately processed in order to obtain isolated RNA or protein extracts, which were

then preserved frozen at -80ºC until further use.

*RNA isolation***.** Total RNA was isolated from cultured cells using the Trizol reagent and following the manufacturer's instructions (Life Technologies, Carlsbad, CA) and previous studies (8; 10; 40; 41). Total RNA concentrations were determined spectrophotometrically using the NanoDrop 1000 (Thermo Scientific, Waltham, MA, USA).

Quantitative real time-PCR amplification (qRT-PCR). TaqMan-minor groove binder (MGB) moiety (TaqMan® primers, fluorescein amidite (FAM) dye labelled, Life Technologies) based real-time polymerase chain reaction (qPCR) reactions were performed using the ABI PRISM® 7900HT Sequence Detector System (Applied BioSystems, Foster City, CA, USA), together with commercially available predesigned primers and probes as shown in Table 1. All the study samples were run in triplicates for all the analyses of each marker.

Protein extraction. Cultured cells were washed with Hanks medium two times and digested with 0.05% trypsin at 37ºC for 10 minutes.

Immunoblotting of 1D electrophoresis. Protein levels of oxidative stress and protein catabolism were explored in the myotubes of both patients and controls using immunoblotting as previously described (8-11; 39-42).

Four fresh 10-well mini-gels were always simultaneously loaded (containing all the study samples) for each of the antigens. Experiments were confirmed twice for the antigens analyzed in the investigation. Proteins were then separated by electrophoresis, transferred to polyvinylidene difluoride (PVDF) membranes, blocked with BSA and incubated overnight with selective primary antibodies. Protein content of different muscle proteins were identified using specific primary antibodies: total malondialdehyde (MDA)-protein adduct formation (1:4000, anti-MDA protein adduct antibody, MD20A-G1b, Academy Bio-Medical Company, Inc., Houston, TX, USA), total ubiquitinated proteins (1:5000, anti-ubiquitin protein antibody, A-100, Boston Biochem, Cambridge, MA, USA), and GAPDH (1:2000, anti-GAPDH antibody, FL-335, Santa Cruz Biotechnology, Santa Cruz, CA, USA). Negative control

experiments in which the primary antibodies were omitted were also conducted in order to assess the specificity of the corresponding antibodies (Figure E2). Accordingly, the bands that did not appear in the negative control immunoblots were measured as the modified proteins (either bound to MDA or ubiquitinated) for the purpose of the study (Figure E2).

Protein degradation, tyrosine release assay. Protein degradation was explored on the basis of the rate of production of free tyrosine from myotube cultures using the specific tyrosine release assay as previously described in tissues (4; 9; 11; 12).

Statistical Analysis

Statistical power was calculated using specific software (StudySize 2.0, CreoStat HB, Frolunda, Sweden). FFMI and QMVC were selected as the target variables to estimate the statistical power in the study. On the basis of a standard power statistics established at a minimum of 80% and assuming an alpha error of 0.05, the statistical power was sufficiently high to detect a minimum difference of eight points between groups (N=9 minimum number of subjects in each group) in the sample size and standard deviation.

Normality of the study variables was checked using the Shapiro-Wilk test. In order to normalize all the results corresponding to gene expression (RT-PCR experiments), a mathematical transformation consisting of the conversion of the actual results into the naperian logarithm was performed for all the experimental groups of myotubes. Clinical and physiological data are expressed as mean (standard deviation) in tables, whereas biological results are represented as linear graphics for each study group and time-point. Several sets of comparisons were performed in the myotubes as described below. Comparisons of the different cohorts of myotubes (non-treated and 1h-, 6h-, and 24h- RNO treatment) between COPD patients and healthy controls were assessed using the unpaired T-test. Furthermore, comparisons between each of the time-cohort (1h, 6h, and 24h) and their respective non-treated controls were also explored for each study group separately (COPD patients and healthy controls) using the paired T-test. Finally, the potential influence of the treatment

effect and the interaction between treatment and disease status was assessed using the analyses of variance (ANOVA) of two factors: disease (COPD patients versus healthy controls) and treatment with RNO in the corresponding experimental groups (time-cohorts: 1h, 6h, and 24h).

RESULTS

Clinical characteristics

Table 2 shows all clinical and functional variables of controls and COPD patients recruited in the study. Age did not significantly differ between patients and healthy controls. Body composition as measured by BMI and FFMI was significantly reduced in COPD patients. Importantly, smoking history did not differ between COPD patients and healthy controls. Compared to healthy controls, COPD patients exhibited severe airflow limitation, functional signs of emphysema, and reduced both exercise capacity and quadriceps strength (Table 2). Moreover, levels of C-reactive protein and fibrinogen were higher in the COPD patients than in healthy controls (Table 2).

Redox signaling in myotubes at baseline and in response to RNO at different time-points

At baseline. No significant differences were observed in the mRNA expression levels of the genes nicotinamide adenine dinucleotide phosphate (NADPH) oxidase (*NOX*) 2 and 4, nuclear factor (erythroid-derived 2)-like 2 (*NRF*2), or NADPH dehydrogenase quinone (*NQO*)1 in the myotubes between patients and healthy controls (Figures 3A-3D). Interestingly, levels of MDA-protein adducts were significantly increased in the myotubes of COPD patients compared to the controls (Figure 4). At baseline, no differences were observed in the levels of mRNA expression of heme oxygenase (*HO*)-1, glutamate-cysteine ligase catalytic (*GCLC*) and GCL modifier (*GCLM*) between patients and controls (Figures 5A-5C). Among the patients a significant positive association was observed between *GCLC* myotube mRNA expression and total blood protein levels (Table 3A).

Effects of RNO treatment. Compared to baseline, mRNA levels of *NOX4* were upregulated in the myotubes of patients at the three time-points (1h, 6h, and 24h), as well as in those of the controls after 6 and 24h of treatment with RNO (Figure 3B), while no differences were seen in *NOX2* mRNA expression (Figure 3A). Interestingly, *NFR2* mRNA expression was also upregulated at 1h- and 6h-time points in the myotubes of the patients, whereas in the control subjects, it was upregulated only after 6h of RNO treatment (Figure 3C). Levels of mRNA expression of *NQO1* was significantly upregulated at 6h-time point compared to baseline in the myotubes of both groups of subjects (Figure 3D). Treatment with RNO for 6h did not induce any significant effect on MDA-protein adducts in the myotubes of either patients or the controls compared to baseline (Figure 4). *HO-1* and *GCLC* mRNA expression was upregulated in the myotubes of both COPD patients and healthy controls after treatment with RNO for 6h (Figures 5A and 5B). Compared to baseline, RNO did not induce any significant effect on *GCLM* mRNA expression in the myotubes of any study group (Figure 5C).

Muscle anabolism signaling in myotubes at baseline and in response to RNO at different time-points

At baseline. No significant differences were observed in the mRNA expression levels of insulin-like growth factor (*IGF*)1, mitochondrial transcription factor A (*TFAM*), myocyte-specific enhancer factor (*MEF*)2C, *Myogenin*, or Myogenic differentiation (*MYOD*) in the myotubes between patients and control subjects (Figures 6A-6E), while mRNA expression levels of peroxisome proliferator-activated receptor-gamma coactivator (*PGC*)*1-alpha* were significantly reduced in the myotubes of the patients (Figure 6F). Myotube mRNA expression levels of *Sirtuin-1*, fibroblast growth factor inducible (*FN*)14, and fibronectin type III domain-containing protein (*FNDC*)5 did not differ between patients and controls (Figures 7A-7C). Significant positive correlations were found between several lung function parameters and myotube mRNA expression levels of *MEF2C*, *Myogenin*, and *FNDC5* among the patients (Table 3A).

Effects of RNO treatment. Compared to baseline, *IGF-1* mRNA expression was upregulated in the myotubes of the 6h-cohort in both patients and control subjects, and the effect was significantly greater in the latter group (Figure 6A). Compared to baseline, *MEF2C* mRNA expression was downregulated in the myotubes treated with RNO for 6h and 24h in both study groups (Figure 6C), whereas no differences were observed in *TFAM* mRNA expression (Figure 6B). *Myogenin* mRNA expression was significantly downregulated in the myotubes after treatment with RNO for 1h, 6h, and 24h in both groups of subjects (Figure 6D). Moreover, in the cells of both patients and controls, *MYOD* mRNA expression was also downregulated after 6h treatment with RNO (Figure 6E). Levels of *PGC-1-alpha* mRNA expression remained significantly lower in the myotubes of the patients after 1h treatment with RNO (Figure 6F). Interestingly, compared to baseline, *Sirtuin-1* and *FN14* mRNA expression levels were upregulated after 6h treatment with RNO in the myotubes of both controls and COPD patients (Figures 7A and 7B). Nonetheless, mRNA expression levels of *FNDC5* were downregulated in the myotubes of both controls and COPD patients after 6h and 24h treatment with RNO, and in the latter group also at 1h time-point (Figure 7C). Among the patients, lung parameters positively correlated with *Myogenin* and *MEF2C* mRNA expression in the myotubes exposed to RNO for 6h (Table 3B).

Muscle catabolism in myotubes at baseline and in response to RNO at different time-points

At baseline. Tyrosine release levels were significantly greater in the myotubes of the patients than in the controls (Figure 8A). Compared to the controls, mRNA expression of *Follistatin* was significantly lower in the myotubes of the patients, while those of *Myostatin* were increased (Figures 8B and 8C, respectively). No significant differences were observed in the myotube mRNA expression levels of *Atrogin-1*, *muscle RING-finger* protein (*MuRF*)-1, or tripartite motif-containing protein (*TRIM)32* between patients and control subjects at baseline (Figures 8D-8F). Total protein ubiquitination levels were significantly higher in the myotubes

of COPD patients than in the controls (Figure 8G). Levels of mRNA expression of the autophagic markers *Microtubule-associated protein 1A/1B-light chain (LC)3B* or *Beclin-1* did not differ between patients and controls (Figures 9A and 9B).

Effects of RNO treatment. After 6h treatment with RNO levels of tyrosine release (proteolysis) were significantly decreased only in the myotubes of the patients compared to baseline, while no differences were detected in the controls (Figure 8A). Compared to baseline, no differences were observed in the mRNA expression levels of *Follistatin* after RNO treatment in either patients or healthy controls (Figure 8B). Furthermore, myotube mRNA expression levels of *Follistatin* were significantly lower in COPD patients than those in the controls in all three time-points (1h, 6h, and 24h) (Figure 8B). Interestingly, mRNA expression levels of *Myostatin*, Atrogin-1, and *MuRF-1* were significantly downregulated in the myotubes of both COPD patients and healthy controls after 6h treatment with RNO (Figures 8C-8E). Additionally, *MuRF-1* mRNA expression was also downregulated at 24h time-point in the myotubes of the patients compared to both baseline and the control subjects (Figure 8E). Interestingly, in the 6h-cohort, mRNA expression of *TRIM32* was also significantly downregulated in the myotubes of the patients (Figure 8F). Treatment with RNO for 6h induced a significant decline in total protein ubiquitination levels only in the myotubes of COPD patients compared to baseline, while no differences were seen in those of the control subjects (Figure 8G). After 1h of RNO treatment, *LC3B* mRNA expression was upregulated in the myotubes of patients and control subjects, and in the latter group, its levels remained higher at the 6h time-point, while no effects were seen in mRNA expression of *Beclin-1* in any of the study groups (Figure 9).

Myosin isoforms in myotubes at baseline and in response to RNO at different time-points

At baseline. Levels of mRNA expression of myosin heavy chain (*MyHC*)-I did not differ between control subjects and COPD patients (Figures 10A-10C), whereas *MyHC-IIa* and

MyHC-IIx mRNA expression levels were significantly downregulated in the myotubes of the latter group (Figures 10B and 10C, respectively).

Effects of RNO treatment. Interestingly, compared to baseline, treatment with RNO for 24h induced a significant upregulation of *MyHC-I* and *MyHC-IIx* mRNA expression in the myotubes of both patients and controls (Figure 10A). Moreover, myotube mRNA expression of the latter isoform was also significantly upregulated in the 1h- and 6h-cohorts of patients (Figure 10C), whereas no significant effects of RNO treatment on *MyHC-IIa* mRNA expression were seen in the myotubes of any study group (Figure 10B). A significant positive correlation was found between *MyHC-I* myotube mRNA expression and diffusion capacity among the COPD patients at 6h time-point (Table 3B).

DISCUSSION

First of all, it should be underscored that relevant findings of part of the study markers analyzed in the study were observed in the myotubes of both COPD patients and healthy subjects as if cAMP signaling induced changes in the expression of genes involved in the regulation of muscle redox balance and metabolism in a rather general fashion irrespective of the underlying disease. Collectively, the findings encountered in the investigation imply that cAMP signaling (roflumilast treatment) for different time-points, especially the 6h-cohort, induced important beneficial effects on muscle metabolism and proteolysis in myotubes of cachectic COPD patients and to some extent also in those of the healthy controls. A discussion of the most important study findings follows below.

In the current investigation, COPD patients exhibited a very severe airway obstruction and functional signs of lung emphysema. Their body composition was severely altered, and they also showed poor exercise capacity and reduced quadriceps muscle strength compared to the control subjects. From a molecular standpoint, the most remarkable findings detected in the myotubes of the cachectic COPD patients were that levels of *Myostatin* and proteolysis as

449 measured through tyrosine release assay significantly decreased in response to increased
450 cAMP signaling for 6 hours, probably as a result of a decline in total protein ubiquitination
451 levels, while oxidative stress (MDA-protein adducts) remained elevated in the myotubes of
452 COPD patients following treatment with roflumilast. Indeed, the significant reduction in
453 muscle proteolysis observed in the myotubes of the COPD patients after six hours of
454 treatment with the PDE4 inhibitor was one of the most striking results in the investigation.
455 Importantly, these results were accompanied by a significant decline in the expression of
456 proteolytic markers such as the atrogenes: *Atrogin-1*, *MuRF-1*, *TRIM32*, total protein
457 ubiquitination levels, and *Myostatin* in the myotubes of COPD patients following 6 hours of
458 treatment with roflumilast. These findings suggest that increased cAMP levels targeted
459 ubiquitin-proteasome pathway leading to lower levels of tyrosine release in the muscles of the
460 patients as a result of the treatment. Another interesting finding was the rise in expression
461 levels of the histone deacetylase *Sirtuin-1* within the myotubes after treatment with
462 roflumilast for six hours. A wide range of beneficial effects are observed in tissues following
463 *Sirtuin-1* protein deacetylase activity through the action of mediators, namely activation of the
464 transcription factors PGC-1alpha (21; 28; 29) and inhibition of FoxO1 and FoxO3 activities
465 (29), which in turn, prevent the activation of atrogenes and autophagy genes. Taken together,
466 it would be possible to conclude that Sirtuin-1 activity also acts as a major player in the
467 roflumilast-induced reduced proteolysis that was detected in the myotubes of patients with
468 advanced COPD. These are very relevant findings with potential clinical applicability in
469 muscles of patients with severe COPD.

470 Similar findings to results reported herein have also been shown in experimental
471 models of muscle wasting and atrophy. As such cAMP-inducing agents were demonstrated to
472 promote an adaptive response in skeletal muscles characterized by an increase in fiber sizes
473 (5). Improvements in muscle function and atrophy were also seen in animal models of disuse,
474 denervation, aging, and muscular dystrophy in response to cAMP signaling induced by

pharmacological agents (5); (25; 26). A decline in ubiquitin-proteasome activity and in the expression of markers of this proteolytic pathway was seen in cultured myotubes obtained from rat skeletal muscles, treated with the phosphodiesterase inhibitor isobutylmethylxanthine (23). In the same cells, isobutylmethylxanthine-induced accumulation of cAMP inactivated transcription factors involved in muscle mass loss and atrophy such as forkhead box O (FoxO)3 (23).

A relevant factor that may have contributed to muscle wasting is hypoxia, especially in the patients. In fact, body and muscle mass loss were identified in experimental models of chronic continuous or intermittent hypoxia (14; 15; 22; 51; 52). Biological mechanisms such as protein synthesis inhibition (38), mitochondrial enzyme alterations (6);(27), aerobic to anaerobic shift due to mitochondrial loss (24), a rise in leptin concentrations, and a decrease in metabolic parameters (sugar and cholesterol) (30) mediate hypoxia-induced body and muscle mass loss as demonstrated in those animal models. On this basis, it is likely that metabolic and mitochondrial alterations through increased oxidative stress levels were important contributors to body and muscle mass loss in the muscles of the patients.

Roflumilast-induced cAMP signaling also favored antioxidant defense through upregulation of the *NRF*2 pathway in muscles of both patients and healthy controls. A significant increase in the expression of the redox signaling enzyme NADPH oxidase subunit *NOX4* was observed in the cultured myotubes treated with roflumilast for six hours in both cachectic COPD patients and healthy controls. *NOX4* produces both superoxide anion and hydrogen peroxide within skeletal muscle fibers. Reactive oxygen species (ROS) synthesized by *NOX4* may act as signaling molecules of muscle growth and regeneration (20). Interestingly, expression levels of the transcription factor *NRF2* were also significantly higher in response to roflumilast treatment for six hours. This is a very relevant finding as *NRF2* regulates the expression of key antioxidant enzymes in skeletal muscles and other cells. Under oxidative stress conditions, it translocates to the nucleus where it binds to a DNA

promoter to start transcription of antioxidant genes such as *NQO1*, *GCLC*, *GCLM*, and *HO-1* (54). In keeping with this, myotube expression levels of the oxidoreductase *NQO1* and that of the *NRF2* targets *HO-1*, *GCLC*, and *GCLM* were also significantly greater in the 6-hour time-cohort of roflumilast treatment compared to baseline in both cachectic patients and healthy controls. Importantly, these enzymes have been shown to scavenge ROS in several models (56; 58; 59). For instance, *NQO1* has been shown to scavenge superoxide anion in cardiovascular and smooth muscle cells in animals and patients (59). They also exert beneficial effects in several experimental models and other cell types (56).

Moreover, activation of *NRF2* is of biological relevance as it plays a crucial role in the detoxification of cells from the damaging effects of oxidants (54). Interestingly, the rise in *NRF2* and its antioxidant targets was seen in the 6h-time cohort of myotubes. In fact, levels of those antioxidant systems were similar to baseline after 24 hours of treatment with roflumilast. These findings suggest that in the current in vitro model, activity of roflumilast active metabolite achieved its peak after six hours of treatment. Indeed, these observations are in line with those reported in patients with COPD, in whom the once-daily dosage (500-microgram tables) reached the maximum concentration of the active N-oxide metabolite in eight hours approximately (57). Taken together, these results imply that the effects of roflumilast are best achieved within the range six- to eight-hour treatment in both in vivo and in vitro models. Whether treatment with roflumilast may improve skeletal muscle mass and function in in vivo models with patients with COPD remains to be elucidated. Trials specifically designed to target this relevant systemic manifestation of COPD should be conducted in the near future.

Another relevant finding was the rise in *IGF-1* expression in the 6h-cohort myotubes. IGF-1 is a highly preserved signaling pathway that mediates protein synthesis and muscle growth. Since patients in the study were severely depleted, treatment with roflumilast appears of interest as *IGF-1* stimulates muscle cell proliferation. In fact, *MyoD* and *Myogenin* levels

were decreased at 6h-time point compared to baseline in the myotubes of both patients and healthy controls. These findings imply that roflumilast is likely to exert its beneficial effects in the early phases of muscle regeneration rather than in late stages.

A switch to a less fatigue-resistant phenotype has been consistently shown in skeletal muscles of the lower limbs in patients with chronic conditions such as COPD (18; 41; 42), in models of disuse muscle atrophy (10; 11), and in cachectic muscles of mice (8; 9; 12). Furthermore, atrophy of muscle fibers, especially of the fast-twitch fibers has been consistently demonstrated in the vastus lateralis of patients with COPD and in muscles of mice exposed to hindlimb unloading (10; 11). In the current investigation, gene expression of the slow- (*MyHC-I*) and fast-twitch (*MyHC-IIx*) myosin isoforms was upregulated in response to roflumilast treatment (24h both isoforms) in the myotubes of severe COPD patients and healthy control subjects. Levels of *MyHC-IIa* were not modified by treatment with the PDE4 inhibitor at any time-point. These are very interesting observations, since muscle atrophy and loss of contractile protein is a major problem in the lower limb muscles of patients with advanced COPD with and without muscle wasting (18; 33; 42). Again, it is likely that the downregulated expression of atrogenes and of other proteolytic markers, including tyrosine release observed as a result of cAMP signaling treatment may account for the increase in *MyHC-I* and *MyHC-IIx* gene expression. As a matter of fact, contractile myosin is a major target for increased muscle protein breakdown in models of muscle atrophy (8-12; 19; 37; 42; 49; 53). These mechanisms may prove useful to preventing lower limb muscles from undergoing further proteolysis in patients with COPD.

Conclusions

In myotubes of severe COPD patients with cachexia, roflumilast-induced cAMP signaling exerts beneficial effects by targeting muscle protein breakdown along with reduced expression of proteolytic markers of the ubiquitin-proteasome system and that of myostatin. Moreover, roflumilast also favored antioxidant defense through upregulation of *NRF*2 and

553 Sirtuin-1 pathways, while it improved the expression of slow- and fast-twitch myosin
554 isoforms in myotubes of patients and controls. These results have potential therapeutic
555 implications as this PDE4 inhibitor is currently available for the treatment of systemic
556 inflammation and exacerbations in patients with severe COPD.
557
558

ACKNOWLEDGMENTS

The authors are very grateful to Dr. Pilar Ausin and MSc Mireia Admetlló for their help with the patient recruitment and clinical information. The authors are also very grateful to Mr. Sergio Mojal for his continuous statistical advice and analyses of the study results and help with the graphical representation. This study has been supported by CIBERES; FIS 14/00713 (FEDER); SAF-2014-54371-R; SEPAR 2016; FUCAP 2016 (Spain); unrestricted grant from TAKEDA (Japan). Dr. Esther Barreiro was a recipient of the ERS COPD Research Award 2008.

Authors' conflicts of interest in relation to the study: None to declare.

AUTHORS' SPECIFIC CONTRIBUTIONS:

Esther Barreiro: Conception and study design, organization of the experiments, statistical analyses, data interpretation, organization of the representation of the study results, intellectual input, and manuscript writing draft and final version

Ester Puig-Vilanova: Organization of the experiments, cell culture experiments, molecular biology experiments, statistical analyses, representation of the study results

Anna Salazar-Degracia: Statistical analyses, representation of the study results, graphical design

Sergi Pascual-Guardia: Recruitment of the candidate patients and healthy controls according to the inclusion/exclusion criteria established in the investigation, sample collection from the study participants

Carme Casadevall: Cell culture experiments, molecular biology experiments

Joaquim Gea: Organization of the experiments, data interpretation, and intellectual input of study results and manuscript draft

585 Reference List
586
587 1. ATS statement: guidelines for the six-minute walk test. *Am J Respir Crit Care Med*
588 166: 111-117, 2002.

589 2. **Barreiro E**. Skeletal Muscle Dysfunction in COPD: Novelties in The Last Decade.
590 *Arch Bronconeumol* 53: 43-44, 2017.

591 3. **Barreiro E, Bustamante V, Cejudo P, Galdiz JB, Gea J, de LP, Martinez-Llorens**
592 **J, Ortega F, Puente-Maestu L, Roca J and Rodriguez-Gonzalez Moro JM**.
593 Guidelines for the evaluation and treatment of muscle dysfunction in patients with
594 chronic obstructive pulmonary disease. *Arch Bronconeumol* 51: 384-395, 2015.

595 4. **Barreiro E, Puig-Vilanova E, Marin-Corral J, Chacon-Cabrera A, Salazar-**
596 **Degracia A, Mateu X, Puente-Maestu L, Garcia-Arumi E, Andreu AL and**
597 **Molina L**. Therapeutic Approaches in Mitochondrial Dysfunction, Proteolysis, and
598 Structural Alterations of Diaphragm and Gastrocnemius in Rats With Chronic Heart
599 Failure. *J Cell Physiol* 231: 1495-1513, 2016.

600 5. **Berdeaux R and Stewart R**. cAMP signaling in skeletal muscle adaptation:
601 hypertrophy, metabolism, and regeneration. *Am J Physiol Endocrinol Metab* 303: E1-
602 17, 2012.

603 6. **Bigard AX, Brunet A, Guezennec CY and Monod H**. Skeletal muscle changes after
604 endurance training at high altitude. *J Appl Physiol (1985)* 71: 2114-2121, 1991.

605 7. **Calverley PM, Sanchez-Toril F, McIvor A, Teichmann P, Bredenbroeker D and**

Fabbri LM. Effect of 1-year treatment with roflumilast in severe chronic obstructive pulmonary disease. *Am J Respir Crit Care Med* 176: 154-161, 2007.

8. **Chacon-Cabrera A, Fermoselle C, Salmela I, Yelamos J and Barreiro E**. MicroRNA expression and protein acetylation pattern in respiratory and limb muscles of Parp-1(-/-) and Parp-2(-/-) mice with lung cancer cachexia. *Biochim Biophys Acta* 1850: 2530-2543, 2015.

9. **Chacon-Cabrera A, Fermoselle C, Urtreger AJ, Mateu-Jimenez M, Diament MJ, De Kier Joffe ED, Sandri M and Barreiro E**. Pharmacological strategies in lung cancer-induced cachexia: effects on muscle proteolysis, autophagy, structure, and weakness. *J Cell Physiol* 229: 1660-1672, 2014.

10. **Chacon-Cabrera A, Gea J and Barreiro E**. Short- and Long-Term Hindlimb Immobilization and Reloading: Profile of Epigenetic Events in Gastrocnemius. *J Cell Physiol* 2016.

11. **Chacon-Cabrera A, Lund-Palau H, Gea J and Barreiro E**. Time-Course of Muscle Mass Loss, Damage, and Proteolysis in Gastrocnemius following Unloading and Reloading: Implications in Chronic Diseases. *PLoS One* 11: e0164951, 2016.

12. **Chacon-Cabrera A, Mateu-Jimenez M, Langohr K, Fermoselle C, Garcia-Arumi E, Andreu AL, Yelamos J and Barreiro E**. Role of PARP activity in lung cancer-induced cachexia: Effects on muscle oxidative stress, proteolysis, anabolic markers, and phenotype. *J Cell Physiol* 232: 3744-3761, 2017.

13. **Corbu A, Scaramozza A, Badiali-DeGiorgi L, Tarantino L, Papa V, Rinaldi R, D'Alessandro R, Zavatta M, Laus M, Lattanzi G and Cenacchi G**. Satellite cell characterization from aging human muscle. *Neurol Res* 32: 63-72, 2010.

14. **de Theije CC, Langen RC, Lamers WH, Gosker HR, Schols AM and Kohler SE**. Differential sensitivity of oxidative and glycolytic muscles to hypoxia-induced muscle atrophy. *J Appl Physiol (1985)* 118: 200-211, 2015.

15. **Dominguez-Alvarez M, Gea J and Barreiro E**. Inflammatory Events and Oxidant Production in the Diaphragm, Gastrocnemius, and Blood of Rats Exposed to Chronic Intermittent Hypoxia: Therapeutic Strategies. *J Cell Physiol* 232: 1165-1175, 2017.

16. **Evans WJ, Morley JE, Argiles J, Bales C, Baracos V, Guttridge D, Jatoi A, Kalantar-Zadeh K, Lochs H, Mantovani G, Marks D, Mitch WE, Muscaritoli M, Najand A, Ponikowski P, Rossi FF, Schambelan M, Schols A, Schuster M, Thomas D, Wolfe R and Anker SD**. Cachexia: a new definition. *Clin Nutr* 27: 793-799, 2008.

17. **Fearon K, Strasser F, Anker SD, Bosaeus I, Bruera E, Fainsinger RL, Jatoi A, Loprinzi C, MacDonald N, Mantovani G, Davis M, Muscaritoli M, Ottery F, Radbruch L, Ravasco P, Walsh D, Wilcock A, Kaasa S and Baracos VE**. Definition and classification of cancer cachexia: an international consensus. *Lancet Oncol* 12: 489-495, 2011.

18. **Fermoselle C, Rabinovich R, Ausin P, Puig-Vilanova E, Coronell C, Sanchez F, Roca J, Gea J and Barreiro E**. Does oxidative stress modulate limb muscle atrophy

in severe COPD patients? *Eur Respir J* 40: 851-862, 2012.

19. **Fermoselle C, Rabinovich R, Ausin P, Puig-Vilanova E, Coronell C, Sanchez F, Roca J, Gea J and Barreiro E**. Does oxidative stress modulate limb muscle atrophy in severe COPD patients? *Eur Respir J* 40: 851-862, 2012.

20. **Ferreira LF and Laitano O**. Regulation of NADPH oxidases in skeletal muscle. *Free Radic Biol Med* 98: 18-28, 2016.

21. **Gerhart-Hines Z, Rodgers JT, Bare O, Lerin C, Kim SH, Mostoslavsky R, Alt FW, Wu Z and Puigserver P**. Metabolic control of muscle mitochondrial function and fatty acid oxidation through SIRT1/PGC-1alpha. *EMBO J* 26: 1913-1923, 2007.

22. **Giordano C, Lemaire C, Li T, Kimoff RJ and Petrof BJ**. Autophagy-associated atrophy and metabolic remodeling of the mouse diaphragm after short-term intermittent hypoxia. *PLoS One* 10: e0131068, 2015.

23. **Goncalves DA, Lira EC, Baviera AM, Cao P, Zanon NM, Arany Z, Bedard N, Tanksale P, Wing SS, Lecker SH, Kettelhut IC and Navegantes LC**. Mechanisms involved in 3',5'-cyclic adenosine monophosphate-mediated inhibition of the ubiquitin-proteasome system in skeletal muscle. *Endocrinology* 150: 5395-5404, 2009.

24. **Howald H, Pette D, Simoneau JA, Uber A, Hoppeler H and Cerretelli P**. Effect of chronic hypoxia on muscle enzyme activities. *Int J Sports Med* 11 Suppl 1: S10-S14, 1990.

667 25. **Kissel JT, McDermott MP, Mendell JR, King WM, Pandya S, Griggs RC and**
668 **Tawil R**. Randomized, double-blind, placebo-controlled trial of albuterol in
669 facioscapulohumeral dystrophy. *Neurology* 57: 1434-1440, 2001.

670 26. **Kissel JT, McDermott MP, Natarajan R, Mendell JR, Pandya S, King WM,**
671 **Griggs RC and Tawil R**. Pilot trial of albuterol in facioscapulohumeral muscular
672 dystrophy. FSH-DY Group. *Neurology* 50: 1402-1406, 1998.

673 27. **Kwast KE and Hand SC**. Acute depression of mitochondrial protein synthesis during
674 anoxia: contributions of oxygen sensing, matrix acidification, and redox state. *J Biol*
675 *Chem* 271: 7313-7319, 1996.

676 28. **Lagouge M, Argmann C, Gerhart-Hines Z, Meziane H, Lerin C, Daussin F,**
677 **Messadeq N, Milne J, Lambert P, Elliott P, Geny B, Laakso M, Puigserver P and**
678 **Auwerx J**. Resveratrol improves mitochondrial function and protects against
679 metabolic disease by activating SIRT1 and PGC-1alpha. *Cell* 127: 1109-1122, 2006.

680 29. **Lee D and Goldberg AL**. SIRT1 protein, by blocking the activities of transcription
681 factors FoxO1 and FoxO3, inhibits muscle atrophy and promotes muscle growth. *J*
682 *Biol Chem* 288: 30515-30526, 2013.

683 30. **Ling Q, Sailan W, Ran J, Zhi S, Cen L, Yang X and Xiaoqun Q**. The effect of
684 intermittent hypoxia on bodyweight, serum glucose and cholesterol in obesity mice.
685 *Pak J Biol Sci* 11: 869-875, 2008.

686 31. **Lynch GS and Ryall JG**. Role of beta-adrenoceptor signaling in skeletal muscle:

implications for muscle wasting and disease. *Physiol Rev* 88: 729-767, 2008.

32. **Maltais F, Decramer M, Casaburi R, Barreiro E, Burelle Y, Debigare R, Dekhuijzen PN, Franssen F, Gayan-Ramirez G, Gea J, Gosker HR, Gosselink R, Hayot M, Hussain SN, Janssens W, Polkey MI, Roca J, Saey D, Schols AM, Spruit MA, Steiner M, Taivassalo T, Troosters T, Vogiatzis I and Wagner PD**. An official American Thoracic Society/European Respiratory Society statement: update on limb muscle dysfunction in chronic obstructive pulmonary disease. *Am J Respir Crit Care Med* 189: e15-e62, 2014.

33. **Marin-Corral J, Minguella J, Ramirez-Sarmiento AL, Hussain SN, Gea J and Barreiro E**. Oxidised proteins and superoxide anion production in the diaphragm of severe COPD patients. *Eur Respir J* 33: 1309-1319, 2009.

34. **Marquis K, Debigare R, Lacasse Y, LeBlanc P, Jobin J, Carrier G and Maltais F**. Midthigh muscle cross-sectional area is a better predictor of mortality than body mass index in patients with chronic obstructive pulmonary disease. *Am J Respir Crit Care Med* 166: 809-813, 2002.

35. **Miravitlles M and Soler-Cataluna JJ**. GOLD in 2017: A View From the Spanish COPD Guidelines (GesCOPD). *Arch Bronconeumol* 53: 89-90, 2017.

36. **Miravitlles M, Soler-Cataluna JJ, Calle M, Molina J, Almagro P, Quintano JA, Trigueros JA, Cosio BG, Casanova C, Antonio RJ, Simonet P, Rigau D, Soriano JB and Ancochea J**. Spanish Guidelines for Management of Chronic Obstructive Pulmonary Disease (GesEPOC) 2017. Pharmacological Treatment of Stable Phase.

Arch Bronconeumol 53: 324-335, 2017.

37. **Powers SK, Kavazis AN and McClung JM**. Oxidative stress and disuse muscle atrophy. *J Appl Physiol (1985)* 102: 2389-2397, 2007.

38. **Preedy VR, Smith DM and Sugden PH**. The effects of 6 hours of hypoxia on protein synthesis in rat tissues in vivo and in vitro. *Biochem J* 228: 179-185, 1985.

39. **Puig-Vilanova E, Aguilo R, Rodriguez-Fuster A, Martinez-Llorens J, Gea J and Barreiro E**. Epigenetic mechanisms in respiratory muscle dysfunction of patients with chronic obstructive pulmonary disease. *PLoS One* 9: e111514, 2014.

40. **Puig-Vilanova E, Ausin P, Martinez-Llorens J, Gea J and Barreiro E**. Do epigenetic events take place in the vastus lateralis of patients with mild chronic obstructive pulmonary disease? *PLoS One* 9: e102296, 2014.

41. **Puig-Vilanova E, Martinez-Llorens J, Ausin P, Roca J, Gea J and Barreiro E**. Quadriceps muscle weakness and atrophy are associated with a differential epigenetic profile in advanced COPD. *Clin Sci (Lond)* 128: 905-921, 2015.

42. **Puig-Vilanova E, Rodriguez DA, Lloreta J, Ausin P, Pascual-Guardia S, Broquetas J, Roca J, Gea J and Barreiro E**. Oxidative stress, redox signaling pathways, and autophagy in cachectic muscles of male patients with advanced COPD and lung cancer. *Free Radic Biol Med* 79C: 91-108, 2014.

43. **Rabe KF, Bateman ED, O'Donnell D, Witte S, Bredenbroker D and Bethke TD**. Roflumilast--an oral anti-inflammatory treatment for chronic obstructive pulmonary

disease: a randomised controlled trial. *Lancet* 366: 563-571, 2005.

44. **Ricciardi R**. Sedentarism: a concept analysis. *Nurs Forum* 40: 79-87, 2005.

45. **Roca J, Burgos F, Barbera JA, Sunyer J, Rodriguez-Roisin R, Castellsague J, Sanchis J, Antoo JM, Casan P and Clausen JL**. Prediction equations for plethysmographic lung volumes. *Respir Med* 92: 454-460, 1998.

46. **Roca J, Rodriguez-Roisin R, Cobo E, Burgos F, Perez J and Clausen JL**. Single-breath carbon monoxide diffusing capacity prediction equations from a Mediterranean population. *Am Rev Respir Dis* 141: 1026-1032, 1990.

47. **Roca J, Sanchis J, Agusti-Vidal A, Segarra F, Navajas D, Rodriguez-Roisin R, Casan P and Sans S**. Spirometric reference values from a Mediterranean population. *Bull Eur Physiopathol Respir* 22: 217-224, 1986.

48. **Ryall JG and Lynch GS**. The potential and the pitfalls of beta-adrenoceptor agonists for the management of skeletal muscle wasting. *Pharmacol Ther* 120: 219-232, 2008.

49. **Salazar-Degracia A, Blanco D, Vila-Ubach M, de BG, de Solorzano CO, Montuenga LM and Barreiro E**. Phenotypic and metabolic features of mouse diaphragm and gastrocnemius muscles in chronic lung carcinogenesis: influence of underlying emphysema. *J Transl Med* 14: 244, 2016.

50. **Seymour JM, Spruit MA, Hopkinson NS, Natanek SA, Man WD, Jackson A, Gosker HR, Schols AM, Moxham J, Polkey MI and Wouters EF**. The prevalence of quadriceps weakness in COPD and the relationship with disease severity. *Eur*

Respir J 36: 81-88, 2010.

51. **Shortt CM, Fredsted A, Chow HB, Williams R, Skelly JR, Edge D, Bradford A and O'Halloran KD**. Reactive oxygen species mediated diaphragm fatigue in a rat model of chronic intermittent hypoxia. *Exp Physiol* 99: 688-700, 2014.

52. **Slot IG, Schols AM, de Theije CC, Snepvangers FJ and Gosker HR**. Alterations in Skeletal Muscle Oxidative Phenotype in Mice Exposed to 3 Weeks of Normobaric Hypoxia. *J Cell Physiol* 231: 377-392, 2016.

53. **Tidball JG and Spencer MJ**. Expression of a calpastatin transgene slows muscle wasting and obviates changes in myosin isoform expression during murine muscle disuse. *J Physiol* 545: 819-828, 2002.

54. **Venugopal R and Jaiswal AK**. Nrf1 and Nrf2 positively and c-Fos and Fra1 negatively regulate the human antioxidant response element-mediated expression of NAD(P)H:quinone oxidoreductase1 gene. *Proc Natl Acad Sci U S A* 93: 14960-14965, 1996.

55. **Vogelmeier CF, Criner GJ, Martinez FJ, Anzueto A, Barnes PJ, Bourbeau J, Celli BR, Chen R, Decramer M, Fabbri LM, Frith P, Halpin DM, Lopez Varela MV, Nishimura M, Roche N, Rodriguez-Roisin R, Sin DD, Singh D, Stockley R, Vestbo J, Wedzicha JA and Agusti A**. Global Strategy for the Diagnosis, Management, and Prevention of Chronic Obstructive Lung Disease 2017 Report: GOLD Executive Summary. *Arch Bronconeumol* 53: 128-149, 2017.

56. **Walsh AC, Feulner JA and Reilly A**. Evidence for functionally significant polymorphism of human glutamate cysteine ligase catalytic subunit: association with glutathione levels and drug resistance in the National Cancer Institute tumor cell line panel. *Toxicol Sci* 61: 218-223, 2001.

57. **Wedzicha JA, Calverley PM and Rabe KF**. Roflumilast: a review of its use in the treatment of COPD. *Int J Chron Obstruct Pulmon Dis* 11: 81-90, 2016.

58. **Zhou X, Wang JL, Lu J, Song Y, Kwak KS, Jiao Q, Rosenfeld R, Chen Q, Boone T, Simonet WS, Lacey DL, Goldberg AL and Han HQ**. Reversal of cancer cachexia and muscle wasting by ActRIIB antagonism leads to prolonged survival. *Cell* 142: 531-543, 2010.

59. **Zhu H, Jia Z, Mahaney JE, Ross D, Misra HP, Trush MA and Li Y**. The highly expressed and inducible endogenous NAD(P)H:quinone oxidoreductase 1 in cardiovascular cells acts as a potential superoxide scavenger. *Cardiovasc Toxicol* 7: 202-211, 2007.

FIGURE LEGENDS

Figure 1

Schematic representation of the different experimental groups performed in the myotubes cultures of both control subjects and COPD patients. Definition of abbreviations: DM, differentiation medium; DMSO, dimethyl sulfoxide; RNA, ribonucleic acid; RNO, Roflumilast N-oxide.

Figure 2

Representative phase-contrast images of myotubes at 5 days after induction of differentiation (top panel). Black arrows indicate multinucleated myotubes. Proliferating myoblasts are represented in the bottom panel. Scale bar: 100 micrometers (4x, left panel) and 50 micrometers (10x, right panel).

Figure 3

A) Linear graphical representation of *NOX2* mRNA levels expressed as the naperian logarithm in the myotubes of the different time-cohorts obtained from the VL of both healthy subjects and COPD patients. Definition of abbreviations: Ln, naperian logarithm; a.u., arbitrary units; RNO, Roflumilast N-oxide; *NOX2*, nicotinamide adenine dinucleotide phosphate (NADPH) oxidase 2; COPD, chronic obstructive pulmonary disease. The statistical analyses (ANOVA test of two factors) corresponding to the treatment and interaction effects are also indicated as actual P values in each figure.

B) Linear graphical representation of *NOX4* mRNA levels expressed as the naperian logarithm in the myotubes of the different time-cohorts obtained from the VL of both healthy subjects and COPD patients. Definition of abbreviations: Ln, naperian logarithm; a.u., arbitrary units; RNO, Roflumilast N-oxide; *NOX4*, nicotinamide adenine dinucleotide phosphate (NADPH) oxidase 4; COPD, chronic obstructive pulmonary disease. Statistical significance is represented as follows: §:$p<0.05$, and

§§:p<0.01 for comparisons between each time-cohort of cells treated with RNO (1h, 6h, 24h) and their respective baseline group. The statistical analyses (ANOVA test of two factors) corresponding to the treatment and interaction effects are also indicated as actual P values in each figure.

C) Linear graphical representation of *NRF2* mRNA levels expressed as the naperian logarithm in the myotubes of the different time-cohorts obtained from the VL of both healthy subjects and COPD patients. Definition of abbreviations: Ln, naperian logarithm; a.u., arbitrary units; RNO, Roflumilast N-oxide; *NRF2*, nuclear factor erythroid 2-related factor 2; COPD, chronic obstructive pulmonary disease. Statistical significance is represented as follows: §:p<0.05, §§:p<0.01, and §§§:p<0.001 for comparisons between each time-cohort of cells treated with RNO (1h, 6h, 24h) and their respective baseline group. The statistical analyses (ANOVA test of two factors) corresponding to the treatment and interaction effects are also indicated as actual P values in each figure.

D) Linear graphical representation of *NQO1* mRNA levels expressed as the naperian logarithm in the myotubes of the different time-cohorts obtained from the VL of both healthy subjects and COPD patients. Definition of abbreviations: Ln, naperian logarithm; a.u., arbitrary units; RNO, Roflumilast N-oxide; *NQO1*, nicotinamide adenine dinucleotide phosphate (NAD(P)H) dehydrogenase quinone 1; COPD, chronic obstructive pulmonary disease. Statistical significance is represented as follows: §:p<0.05, and §§§:p<0.001 for comparisons between each time-cohort of cells treated with RNO (1h, 6h, 24h) and their respective baseline group. The statistical analyses (ANOVA test of two factors) corresponding to the treatment and interaction effects are also indicated as actual P values in each figure.

Figure 4

Representative immunoblots of MDA-protein adduct levels (left panel) in the myotubes of two different time-point groups (baseline and 6h-RNO) in both healthy controls and COPD patients. Arrows indicate the measured bands. GAPDH is shown as the loading control. Mean values and standard deviation of total MDA-protein adducts (right panel) as measured by optical densities in arbitrary units (OD, a.u.). Definition of abbreviations: MDA, malondialdehyde; MW, molecular weights; kDa, kilodaltons; RNO, Roflumilast N-oxide; COPD, chronic obstructive pulmonary disease; GAPDH, glyceraldehyde-3-phosphate dehydrogenase; OD, optical densities; a.u., arbitrary units; n.s., non-significant. Statistical significance is represented as follows: *:$p<0.05$, and ***:$p<0.001$ between COPD patients and healthy controls.

Figure 5

A) Linear graphical representation of *HO-1* mRNA levels expressed as the naperian logarithm in the myotubes of the different time-cohorts obtained from the VL of both healthy subjects and COPD patients. Definition of abbreviations: Ln, naperian logarithm; a.u., arbitrary units; RNO, Roflumilast N-oxide; *HO-1*, heme oxygenase-1; COPD, chronic obstructive pulmonary disease. Statistical significance is represented as follows: §§§:$p<0.001$ for comparisons between each time-cohort of cells treated with RNO (1h, 6h, 24h) and their respective baseline group. The statistical analyses (ANOVA test of two factors) corresponding to the treatment and interaction effects are also indicated as actual P values in each figure.

B) Linear graphical representation of *GCLC* mRNA levels expressed as the naperian logarithm in the myotubes of the different time-cohorts obtained from the VL of both healthy subjects and COPD patients. Definition of abbreviations: Ln, naperian logarithm; a.u., arbitrary units; RNO, Roflumilast N-oxide; *GCLC*, glutamate-cysteine ligase catalytic; COPD, chronic obstructive pulmonary disease. Statistical significance is represented as follows: §:$p<0.05$ and §§§:$p<0.001$ for comparisons between each

time-cohort of cells treated with RNO (1h, 6h, 24h) and their respective baseline group. The statistical analyses (ANOVA test of two factors) corresponding to the treatment and interaction effects are also indicated as actual P values in each figure.

C) Linear graphical representation of *GCLM* mRNA levels expressed as the naperian logarithm in the myotubes of the different time-cohorts obtained from the VL of both healthy subjects and COPD patients. Definition of abbreviations: Ln, naperian logarithm; a.u., arbitrary units; RNO, Roflumilast N-oxide; *GCLM*, glutamate-cysteine ligase modifier; COPD, chronic obstructive pulmonary disease. The treatment and interaction effect statistical analyses from the ANOVA test of 2 factors is also indicated in each figure as actual p-values.

Figure 6

A) Linear graphical representation of *IGF-1* mRNA levels expressed as the naperian logarithm in the myotubes of the different time-cohorts obtained from the VL of both healthy subjects and COPD patients. Definition of abbreviations: Ln, naperian logarithm; a.u., arbitrary units; RNO, Roflumilast N-oxide; *IGF-1*, insulin-like growth factor-1; COPD, chronic obstructive pulmonary disease. Statistical significance is represented as follows: *:$p<0.05$ for comparisons between COPD patients and the controls for each time-point; §§§:$p<0.001$ for comparisons between each time-cohort of cells treated with RNO (1h, 6h, 24h) and their respective baseline group. The statistical analyses (ANOVA test of two factors) corresponding to the treatment and interaction effects are also indicated as actual P values in each figure.

B) Linear graphical representation of *TFAM* mRNA levels expressed as the naperian logarithm in the myotubes of the different time-cohorts obtained from the VL of both healthy subjects and COPD patients. Definition of abbreviations: Ln, naperian logarithm; a.u., arbitrary units; RNO, Roflumilast N-oxide; *TFAM*, transcription factor A mitochondrial; COPD, chronic obstructive pulmonary disease. The statistical

analyses (ANOVA test of two factors) corresponding to the treatment and interaction effects are also indicated as actual P values in each figure.

C) Linear graphical representation of *MEF2C* mRNA levels expressed as the naperian logarithm in the myotubes of the different time-cohorts obtained from the VL of both healthy subjects and COPD patients. Definition of abbreviations: Ln, naperian logarithm; a.u., arbitrary units; RNO, Roflumilast N-oxide; *MEF2C*, myocyte enhancer factor-2; COPD, chronic obstructive pulmonary disease. Statistical significance is represented as follows: §:$p<0.05$, and §§:$p<0.01$ for comparisons between each time-cohort of cells treated with RNO (1h, 6h, 24h) and their respective baseline group. The statistical analyses (ANOVA test of two factors) corresponding to the treatment and interaction effects are also indicated as actual P values in each figure.

D) Linear graphical representation of *Myogenin* mRNA levels expressed as the naperian logarithm in the myotubes of the different time-cohorts obtained from the VL of both healthy subjects and COPD patients. Definition of abbreviations: Ln, naperian logarithm; a.u., arbitrary units; RNO, Roflumilast N-oxide; COPD, chronic obstructive pulmonary disease. Statistical significance is represented as follows: §:$p<0.05$, §§:$p<0.01$, and §§§:$p<0.001$ for comparisons between each time-cohort of cells treated with RNO (1h, 6h, 24h) and their respective baseline group. The statistical analyses (ANOVA test of two factors) corresponding to the treatment and interaction effects are also indicated as actual P values in each figure.

E) Linear graphical representation of *MYOD* mRNA levels expressed as the naperian logarithm in the myotubes of the different time-cohorts obtained from the VL of both healthy subjects and COPD patients. Definition of abbreviations: Ln, naperian logarithm; a.u., arbitrary units; RNO, Roflumilast N-oxide; *MYOD*, myogenic differentiation; COPD, chronic obstructive pulmonary disease. Statistical significance

is represented as follows: §:p<0.05, and §§:p<0.01 for comparisons between each time-cohort of cells treated with RNO (1h, 6h, 24h) and their respective baseline group. The statistical analyses (ANOVA test of two factors) corresponding to the treatment and interaction effects are also indicated as actual P values in each figure.

F) Linear graphical representation of *PGC-1-alpha* mRNA levels expressed as the naperian logarithm in the myotubes of the different time-cohorts obtained from the VL of both healthy subjects and COPD patients. Definition of abbreviations: Ln, naperian logarithm; a.u., arbitrary units; RNO, Roflumilast N-oxide; *PGC-1-alpha*, peroxisome proliferator-activated receptor-gamma coactivator-1alpha; COPD, chronic obstructive pulmonary disease. Statistical significance is represented as follows: *:p<0.05 for comparisons between COPD patients and the controls for each time-point. The statistical analyses (ANOVA test of two factors) corresponding to the treatment and interaction effects are also indicated as actual P values in each figure.

Figure 7

A) Linear graphical representation of *Sirtuin-1* mRNA levels expressed as the naperian logarithm in the myotubes of the different time-cohorts obtained from the VL of both healthy subjects and COPD patients. Definition of abbreviations: Ln, naperian logarithm; a.u., arbitrary units; RNO, Roflumilast N-oxide; COPD, chronic obstructive pulmonary disease. Statistical significance is represented as follows: §§:p<0.01 for comparisons between each time-cohort of cells treated with RNO (1h, 6h, 24h) and their respective baseline group. The statistical analyses (ANOVA test of two factors) corresponding to the treatment and interaction effects are also indicated as actual P values in each figure.

B) Linear graphical representation of *FN14* mRNA levels expressed as the naperian logarithm in the myotubes of the different time-cohorts obtained from the VL of both healthy subjects and COPD patients. Definition of abbreviations: Ln, naperian

logarithm; a.u., arbitrary units; RNO, Roflumilast N-oxide; *FN14*, fibroblast growth factor inducible 14; COPD, chronic obstructive pulmonary disease. Statistical significance is represented as follows: §:$p<0.05$ for comparisons between each time-cohort of cells treated with RNO (1h, 6h, 24h) and their respective baseline group. The statistical analyses (ANOVA test of two factors) corresponding to the treatment and interaction effects are also indicated as actual P values in each figure.

C) Linear graphical representation of *FNDC5* mRNA levels expressed as the naperian logarithm in the myotubes of the different time-cohorts obtained from the VL of both healthy subjects and COPD patients. Definition of abbreviations: Ln, naperian logarithm; a.u., arbitrary units; RNO, Roflumilast N-oxide; *FNDC5*, fibronectin type III domain containing 5; COPD, chronic obstructive pulmonary disease. Statistical significance is represented as follows: §§:$p<0.01$, and §§§:$p<0.001$ for comparisons between each time-cohort of cells treated with RNO (1h, 6h, 24h) and their respective baseline group. The statistical analyses (ANOVA test of two factors) corresponding to the treatment and interaction effects are also indicated as actual P values in each figure.

Figure 8

A) Mean values and standard deviation of tyrosine release (tyrosine release assay, nmol/2h) measurements in the baseline and six-hour RNO cohort myotubes of both COPD patients and healthy controls. Definition of abbreviations: nmol, nanomole; h, hour; n.s., non-significant; COPD, chronic obstructive pulmonary disease; RNO, Roflumilast N-oxide. Statistical significance is represented as follows: ***:$p<0.001$ between COPD patients and healthy controls; §§:$p<0.01$ between 6h-RNO treatment and their respective baseline group.

B) Linear graphical representation of *Follistatin* mRNA levels expressed as the naperian logarithm in the myotubes of the different time-cohorts obtained from the VL of both

healthy subjects and COPD patients. Definition of abbreviations: Ln, naperian logarithm; a.u., arbitrary units; RNO, Roflumilast N-oxide; COPD, chronic obstructive pulmonary disease. Statistical significance is represented as follows: *:$p<0.05$, and **:$p<0.01$ for comparisons between COPD patients and the controls for each time-point. The statistical analyses (ANOVA test of two factors) corresponding to the treatment and interaction effects are also indicated as actual P values in each figure.

C) Linear graphical representation of *Myostatin* mRNA levels expressed as the naperian logarithm in the myotubes of the different time-cohorts obtained from the VL of both healthy subjects and COPD patients. Definition of abbreviations: Ln, naperian logarithm; a.u., arbitrary units; RNO, Roflumilast N-oxide; COPD, chronic obstructive pulmonary disease. Statistical significance is represented as follows: *:$p<0.05$ for comparisons between COPD patients and the controls for each time-point; §:$p<0.05$, and §§§:$p<0.001$ for comparisons between each time-cohort of cells treated with RNO (1h, 6h, 24h) and their respective baseline group. The statistical analyses (ANOVA test of two factors) corresponding to the treatment and interaction effects are also indicated as actual P values in each figure.

D) Linear graphical representation of *Atrogin-1* mRNA levels expressed as the naperian logarithm in the myotubes of the different time-cohorts obtained from the VL of both healthy subjects and COPD patients. Definition of abbreviations: Ln, naperian logarithm; a.u., arbitrary units; RNO, Roflumilast N-oxide; COPD, chronic obstructive pulmonary disease. Statistical significance is represented as follows: §§§:$p<0.001$ for comparisons between each time-cohort of cells treated with RNO (1h, 6h, 24h) and their respective baseline group. The statistical analyses (ANOVA test of two factors) corresponding to the treatment and interaction effects are also indicated as actual P values in each figure.

E) Linear graphical representation of *MuRF-1* mRNA levels expressed as the naperian logarithm in the myotubes of the different time-cohorts obtained from the VL of both healthy subjects and COPD patients. Definition of abbreviations: Ln, naperian logarithm; a.u., arbitrary units; RNO, Roflumilast N-oxide; *MuRF-1*, muscle RING-finger protein-1; COPD, chronic obstructive pulmonary disease. Statistical significance is represented as follows: *:$p<0.05$ for comparisons between COPD patients and the controls for each time-point; §:$p<0.05$, §§:$p<0.01$, and §§§:$p<0.001$ for comparisons between each time-cohort of cells treated with RNO (1h, 6h, 24h) and their respective baseline group. The statistical analyses (ANOVA test of two factors) corresponding to the treatment and interaction effects are also indicated as actual P values in each figure.

F) Linear graphical representation of *TRIM32* mRNA levels expressed as the naperian logarithm in the myotubes of the different time-cohorts obtained from the VL of both healthy subjects and COPD patients. Definition of abbreviations: Ln, naperian logarithm; a.u., arbitrary units; RNO, Roflumilast N-oxide; *TRIM32*, tripartite motif-containing protein 32; COPD, chronic obstructive pulmonary disease. Statistical significance is represented as follows: *:$p<0.05$ for comparisons between COPD patients and the controls for each time-point. The statistical analyses (ANOVA test of two factors) corresponding to the treatment and interaction effects are also indicated as actual P values in each figure.

G) Representative immunoblots of total protein ubiquitination (right panel) in the myotubes of two different time-point groups (baseline and 6h-RNO) in both healthy controls and COPD patients. GAPDH is shown as the loading control. Arrows indicate the measured bands. Mean values and standard deviation of total protein ubiquitination (left panel) as measured by optical densities in arbitrary units (OD, a.u.). Definition of abbreviations: MW, molecular weights; kDa, kilodaltons; RNO,

Roflumilast N-oxide; COPD, chronic obstructive pulmonary disease; GAPDH, glyceraldehyde-3-phosphate dehydrogenase; OD, optical densities; a.u., arbitrary units; n.s., non-significant. Statistical significance is represented as follows: *:p<0.05 between COPD patients and healthy controls; §:p<0.05 between 6h-RNO treatment and their respective baseline group.

Figure 9

A) Linear graphical representation of *LC3B* mRNA levels expressed as the naperian logarithm in the myotubes of the different time-cohorts obtained from the VL of both healthy subjects and COPD patients. Definition of abbreviations: Ln, naperian logarithm; a.u., arbitrary units; RNO, Roflumilast N-oxide; *LC3B*, microtubule-associated protein 1A/1B-light chain 3; COPD, chronic obstructive pulmonary disease. Statistical significance is represented as follows: §:p<0.05, §§:p<0.01, and §§§:p<0.001 for comparisons between each time-cohort of cells treated with RNO (1h, 6h, 24h) and their respective baseline group. The statistical analyses (ANOVA test of two factors) corresponding to the treatment and interaction effects are also indicated as actual P values in each figure.

B) Linear graphical representation of *Beclin-1* mRNA levels expressed as the naperian logarithm in the myotubes of the different time-cohorts obtained from the VL of both healthy subjects and COPD patients. Definition of abbreviations: Ln, naperian logarithm; a.u., arbitrary units; RNO, Roflumilast N-oxide; COPD, chronic obstructive pulmonary disease. The statistical analyses (ANOVA test of two factors) corresponding to the treatment and interaction effects are also indicated as actual P values in each figure.

Figure 10

A) Linear graphical representation of *MyHC-I* mRNA levels expressed as the naperian logarithm in the myotubes of the different time-cohorts obtained from the VL of both

healthy subjects and COPD patients. Definition of abbreviations: Ln, naperian logarithm; a.u., arbitrary units; RNO, Roflumilast N-oxide; *MyHC-I*, myosin heavy chain type I; COPD, chronic obstructive pulmonary disease. Statistical significance is represented as follows: §:$p<0.05$, and §§§:$p<0.001$ for comparisons between each time-cohort of cells treated with RNO (1h, 6h, 24h) and their respective baseline group. The statistical analyses (ANOVA test of two factors) corresponding to the treatment and interaction effects are also indicated as actual P values in each figure.

B) Linear graphical representation of *MyHC-IIa* mRNA levels expressed as the naperian logarithm in the myotubes of the different time-cohorts obtained from the VL of both healthy subjects and COPD patients. Definition of abbreviations: Ln, naperian logarithm; a.u., arbitrary units; RNO, Roflumilast N-oxide; *MyHC-IIa*, myosin heavy chain type IIa; COPD, chronic obstructive pulmonary disease. Statistical significance is represented as follows: *:$p<0.05$ for comparisons between COPD patients and the controls for each time-point. The statistical analyses (ANOVA test of two factors) corresponding to the treatment and interaction effects are also indicated as actual P values in each figure.

C) Linear graphical representation of *MyHC-IIx* mRNA levels expressed as the naperian logarithm in the myotubes of the different time-cohorts obtained from the VL of both healthy subjects and COPD patients. Definition of abbreviations: Ln, naperian logarithm; a.u., arbitrary units; RNO, Roflumilast N-oxide; *MyHC-IIx*, myosin heavy chain type IIx; COPD, chronic obstructive pulmonary disease. Statistical significance is represented as follows: *:$p<0.05$ for comparisons between COPD patients and the controls for each time-point; §:$p<0.05$ for comparisons between each time-cohort of cells treated with RNO (1h, 6h, 24h) and their respective baseline group. The statistical analyses (ANOVA test of two factors) corresponding to the treatment and interaction effects are also indicated as actual P values in each figure.

Table 1. Probes used for the quantitative analyses of the target genes in the myotube samples obtained from both COPD patients and healthy controls.

	Gene symbol	Assay ID	Genbank accession number	Target gene
Redox signaling markers	CYBB	Hs00166163_m1	NM_000397.3	*NOX2*
	NOX4	Hs00418356_m1	NM_016931.3	*NOX4*
	NFE2L2	Hs00232352_m1	NM_001145412.2	*NRF2*
	NQO1	Hs00168547_m1	NM_001025433.1	*NQO1*
	HMOX1	Hs00157965_m1	NM_002133.2	*HO-1*
	GCLC	Hs00155249_m1	NM_001197115.1	*GCLC*
	GCLM	Hs00157694_m1	NM_002061.2	*GCLM*
Muscle repair and anabolism markers	IGF1	Hs00153126_m1	NM_001111283.1	*IGF-1*
	TFAM	H200273372_s1	NM_001270782.1	*TFAM*
	MEF2C	Hs00231149_m1	NM_001131005.1	*MEF2C*
	MYOG	Hs01072232_m1	NM_002479.5	*Myogenin*
	MYOD1	Hs00159528_m1	NM_002478.4	*MYOD*
	PPARGC1A	Hs01016719_m1	NM_013261.3	*PGC-1-alpha*
	SIRT1	Hs01009005_m1	NM_001142498.1	*Sirtuin-1*
	TNFRSF12A	Hs00171993_m1	NM_016639.2	*FN14*
	FNDC5	Hs00401006_m1	NM_153756.2	*FNDC5*
Muscle catabolism markers	FST	Hs00246256_m1	NM_013409.1	*Follistatin*
	MSTN	Hs00976237_m1	NM_005259.2	*Myostatin*
	FBXO32	Hs01041408_m1	NM_148177.2	*Atrogin-1*
	TRIM63	Hs00261590_m1	NM_032588.3	*MuRF-1*
	TRIM32	Hs00705875_s1	NM_001099679.1	*TRIM32*
	MAP1LC3B	Hs00917683_m1	BC045759.1	*LC3B*
	AMBRA1	Hs00387943_m1	NM_017749.3	*Beclin-1*
Muscle phenotype markers	MYH7	Hs00165276_m1	NM_000257.2	*MyHC-I*
	MYH2	Hs00430042_m1	NM_017534.5	*MyHC-IIa*
	MYH1	Hs00428600_m1	NM_005963.3	*MyHC-IIx*
Housekeeping gene	GAPDH	Hs99999905_m1	NM_002046.4	*GAPDH*

Abbreviations: ID, identification; hsa, homo sapiens; miR, microRNA; MIMAT, mature microRNA; snRNA, small nuclear RNA; NR, non-coding RNA RefSeq database category; Hs, homo sapiens; m1,

multi-exonic gene assay does not detect genomic DNA; NM, mRNA RefSeq database category; CYBB, cytochrome b-245, beta polypeptide; NOX, NADPH oxidase; NFE2L, nuclear factor, erythroid 2-like; NQO, NAD(P)H dehydrogenase, quinone; HMOX, heme oxygenase; GCLC, glutamate-cysteine ligase, catalytic subunit; GCLM, glutamate-cysteine ligase, modifier subunit; IGF, insulin-like growth factor; TFAM, mitochondrial transcription factor A; s1, single-exon gene assay may detect genomic DNA if present in the sample; MEF, myocyte-enhancer factor; MYOG, myogenin; MYOD, myogenic differentiation; PPARGC1A, Peroxisome proliferator-activated receptor gamma coactivator 1-alpha; SIRT, sirtuin; TNFRSF12A, tumor necrosis factor receptor superfamily, member 12A; FNDC5, fibronectin type III domain containing protein 5; FST, follistatin; MSTN, myostatin; FBXO32, F-Box Protein 32; TRIM, Tripartite motif-containing protein; MAP1LC3B, microtubule-associated protein 1 light chain 3 beta; AMBRA, autophagy/beclin-1 regulator; MYH, myosin heavy chain; and GAPDH, glyceraldehyde-3-phosphate dehydrogenase.

Table 2. Clinical characteristics of cachectic COPD patients and healthy controls.

	Controls	COPD
	N = 10	N = 10
Anthropometry		
Age (years)	61 (7)	66 (10)
BMI (kg/m^2)	27 (2)	19 (2) ***
FFMI (kg/m^2)	19 (2)	15 (1) ***
Smoking History		
Active, N, %	0,0	4,40
Ex-smoker, N, %	5,50	6,60
Never smoker, N, %	5,50	0,0
Pack-years	60 (18)	60 (21)
Lung function		
FEV_1 (% pred)	95 (8)	35 (14) ***
FVC (% pred)	93 (7)	62 (19) ***
FEV_1/FVC (%)	75 (3)	42 (13) ***
RV (% pred)	115 (15)	211 (63) **
TLC (% pred)	105 (11)	119 (18)
RV/TLC (%)	42 (3)	65 (12) ***
DLco (% pred)	100 (16)	48 (17) ***
K_{CO} (% pred)	92 (14)	59 (17) ***
PaO_2 (kPa)	11.3 (0.4)	9.4 (1.7) **
$PaCO_2$ (kPa)	5.6 (0.6)	5.8 (0.7)
Exercise capacity & muscle force		
Six-minute walking test (m)	526 (47)	400 (142)*
QMVC (kg)	42 (11)	30 (10)*
Blood parameters		
Albumin (g/dL)	4.5 (0.4)	4.9 (0.9)
Total proteins (g/dL)	6.2 (1.6)	6.5 (1.4)
CRP (mg/dL)	0.2 (0.06)	5.3 (5.2)*
Fibrinogen (mg/dL)	348 (95)	498 (100)*
GSV (mm/h)	15 (8)	15 (7)

Values are expressed as mean (standard deviation).

Abbreviations: COPD, chronic obstructive pulmonary disease; N, number of patients; kg, kilograms; cm, centimeters; m, meters; BMI, body mass index; FFMI, fat-free mass index; FEV_1, forced expiratory volume in one second; pred, predicted; FVC, forced vital capacity; RV, residual volume; TLC, total lung capacity; DLco, carbon monoxide transfer; K_{CO}, *Krough* transfer factor; PaO_2, arterial oxygen partial pressure; $PaCO_2$, arterial carbon dioxide partial pressure; QMVC, quadriceps maximal velocity contraction; g, grams; dL, deciliter; mg, miligrams.; CRP, C-reactive protein; GSV, globular sedimentation velocity; mm, millimeters; h, hour.

Statistical significance: *, $p \leq 0.05$, **, $p \leq 0.01$, ***, $p \leq 0.001$ between COPD patients and control subjects.

Ta Table 3. Significant correlations of study variables in the myotubes of the cachectic COPD pat patients.

A. Non-treated myotubes (baseline group)				
	FEV_1	**DLco**	**Kco**	**Total proteins**
MEF2C	r=0.725 p=0.018	r=0.763 p=0.017		
Myogenin			r=0.762 p=0.017	
FNDC5			r=0.714 p=0.031	
GCLC				r=0.715 p=0.030

B. Myotubes exposed to 6h-RNO treatment		
	FEV_1	**DLco**
MEF2C	r=0.706 p=0.022	
Myogenin		r=0.691 p=0.039
MyHC-I		r=0.787 p=0.012

For the sake of clarity in the table, units have been omitted as they are already being shown in the corresponding figures and tables.

Abbreviations: COPD, chronic obstructive pulmonary disease; FEV_1, forced expiratory volume in one second; DLco, carbon monoxide transfer; K_{CO}, *Krough* transfer factor; *MEF*, myocyte enhancer factor; *FNDC5*, fibronectin type III domain containing protein 5; *GCLC*, glutamate-cysteine ligase, catalytic; RNO, roflumilast N-oxide; *MyHC-I*, myosin heavy chain – type I.

Barreiro E. et al. Figure 1

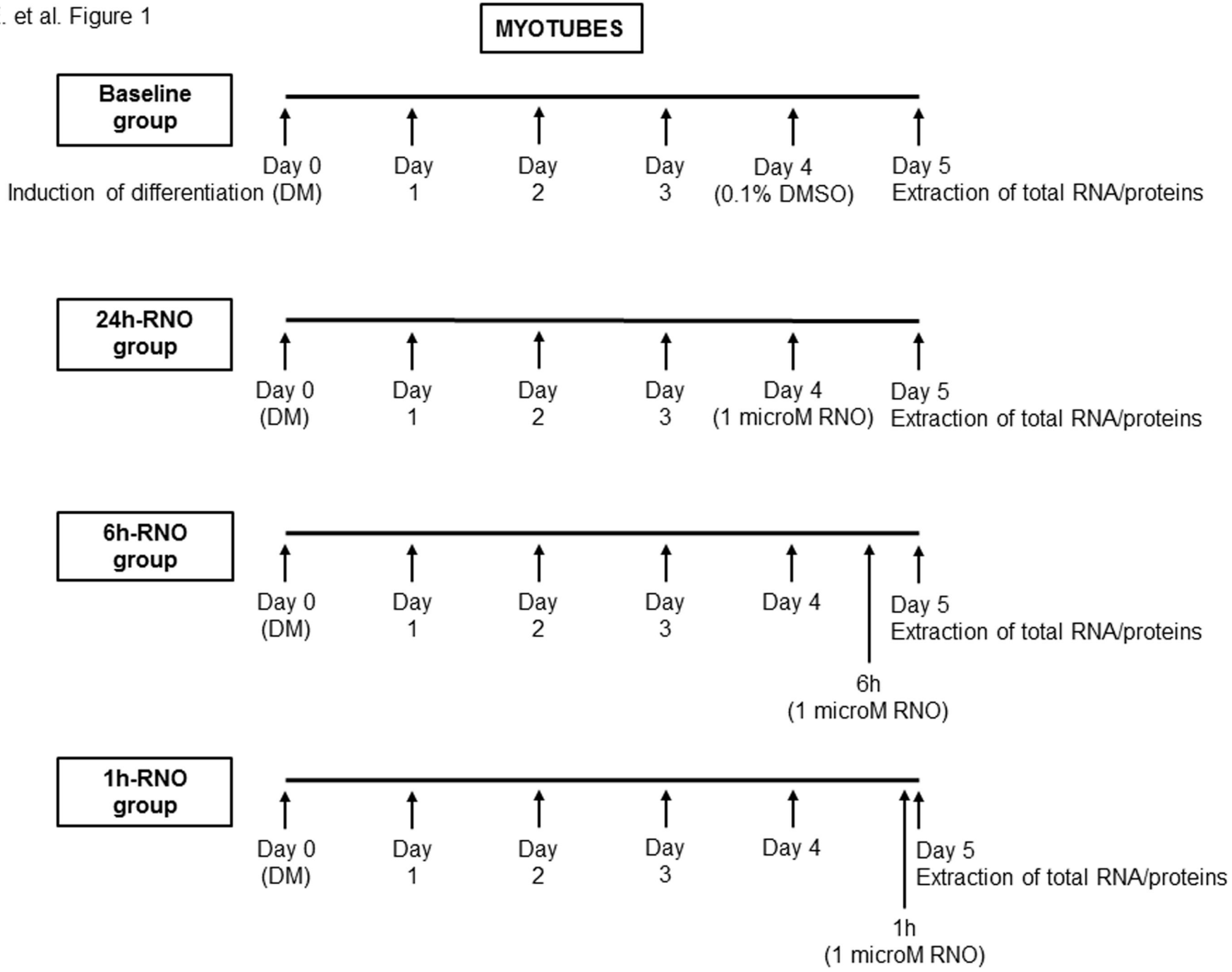

Barreiro E. et al. Figure 2

MYOTUBES

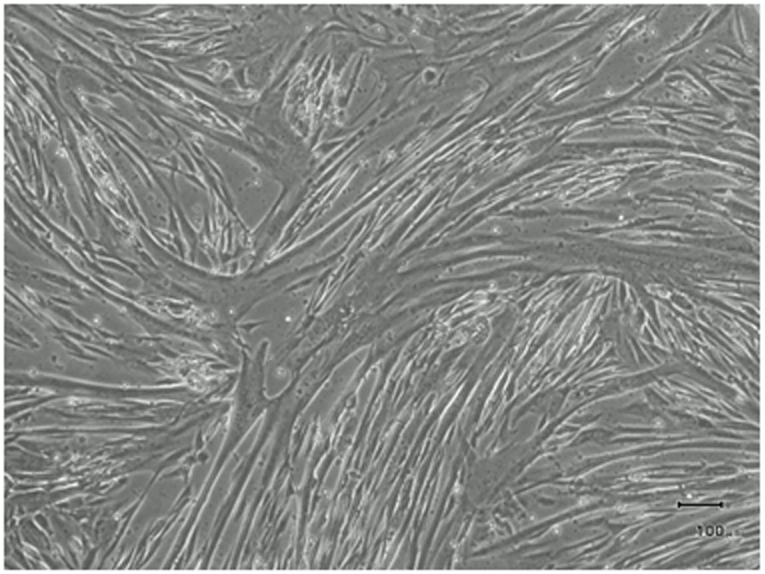

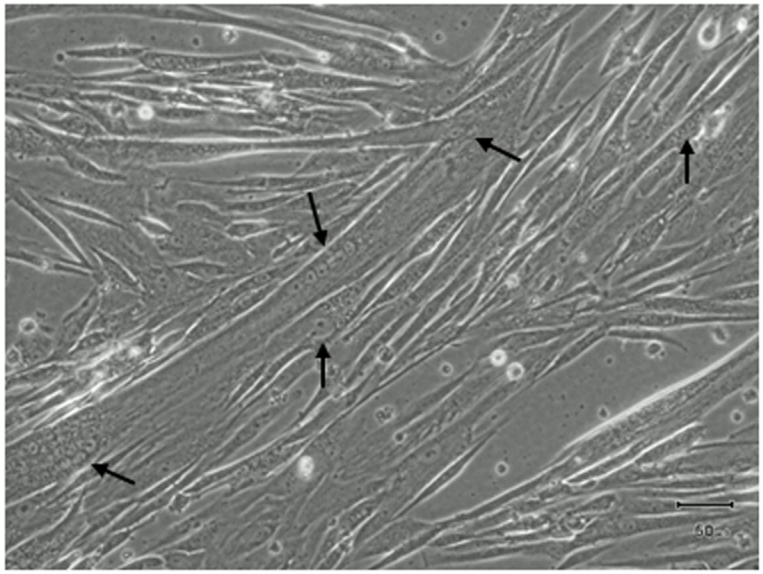

MYOBLASTS

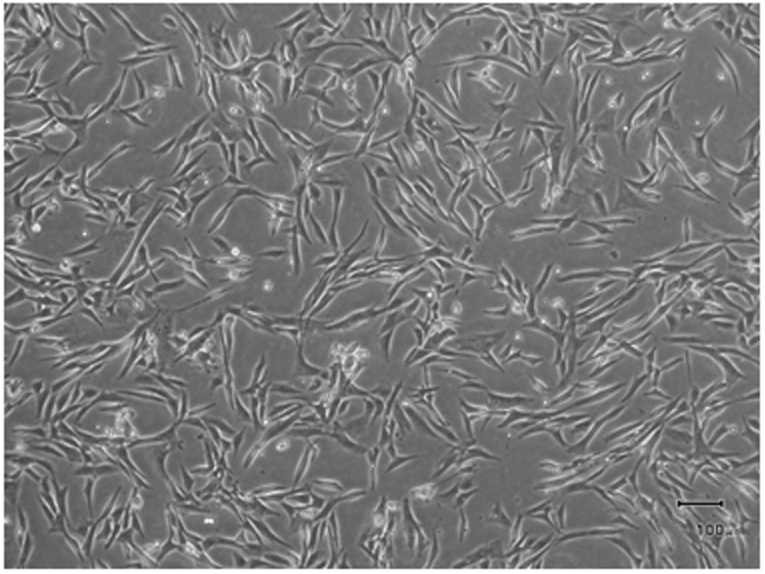

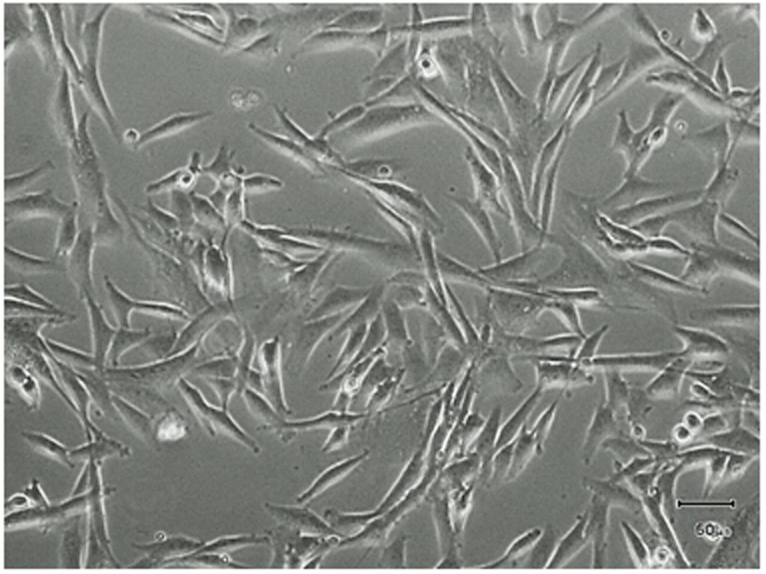

Barreiro E. et al. Figure 3

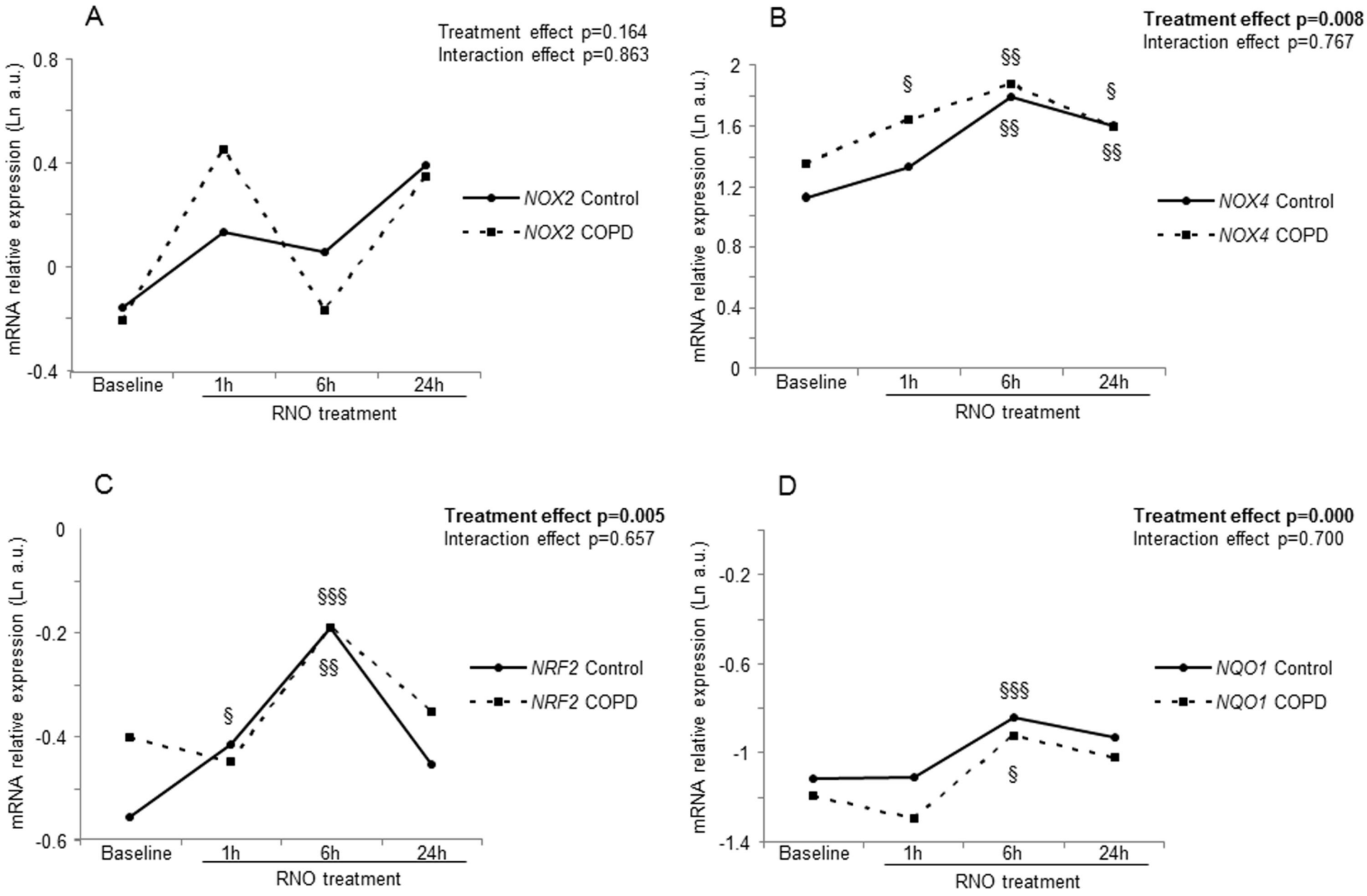

Barreiro E. et al. Figure 4

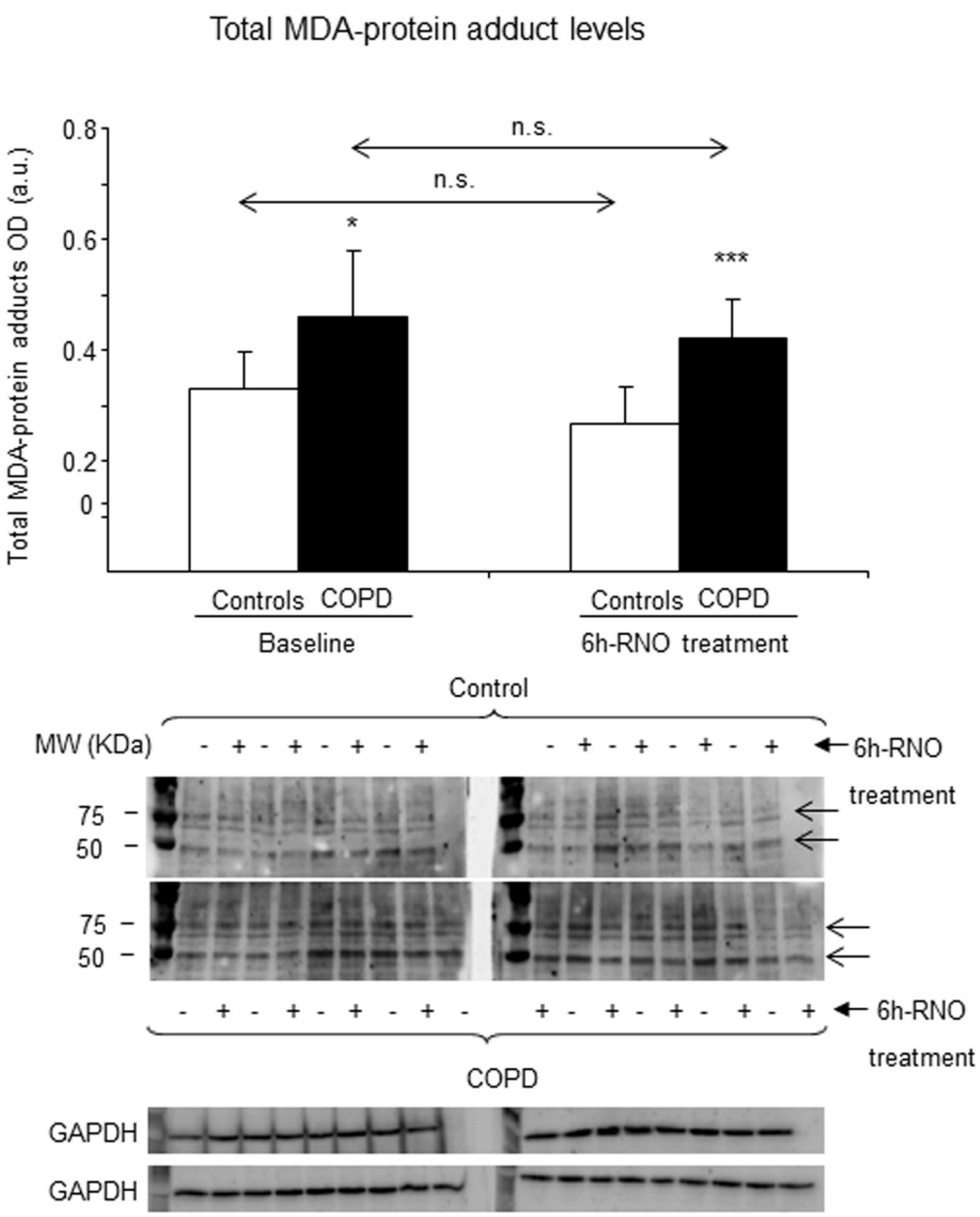

Barreiro E. et al. Figure 5

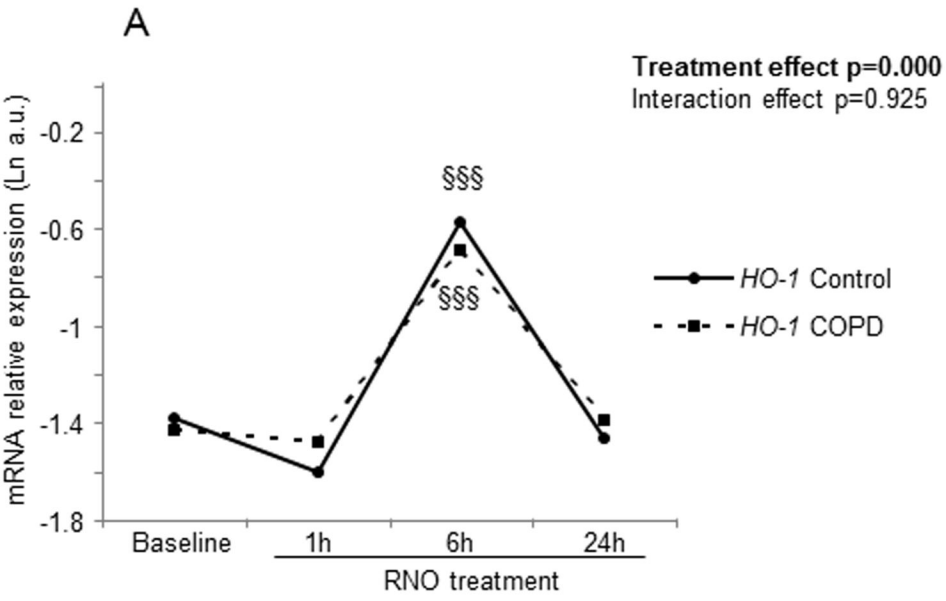

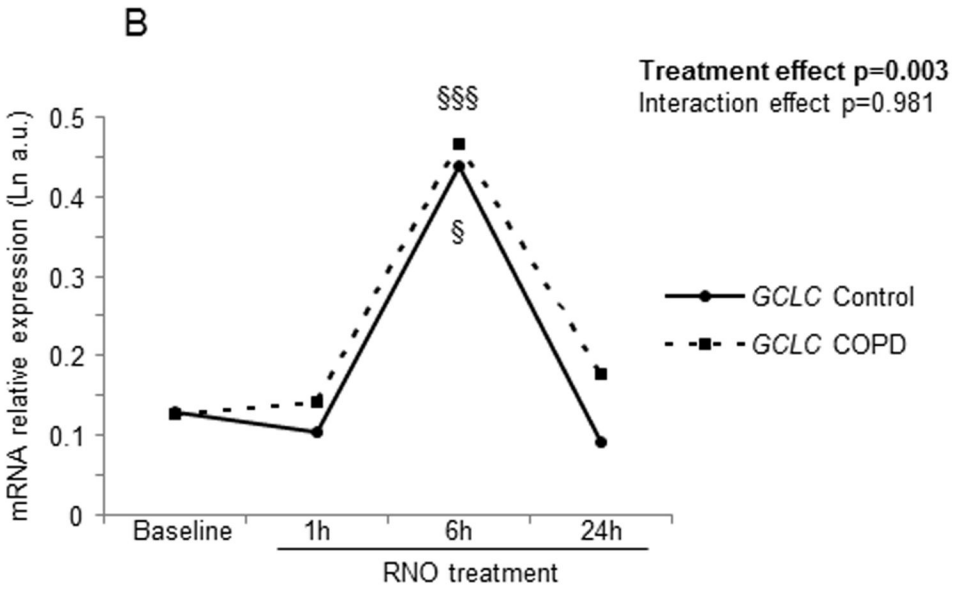

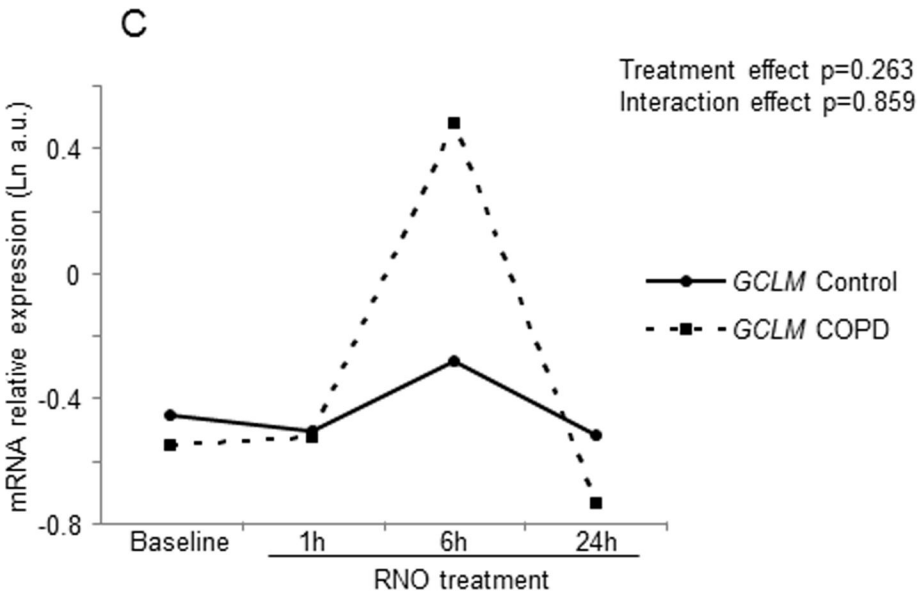

Barreiro E. et al. Figure 6

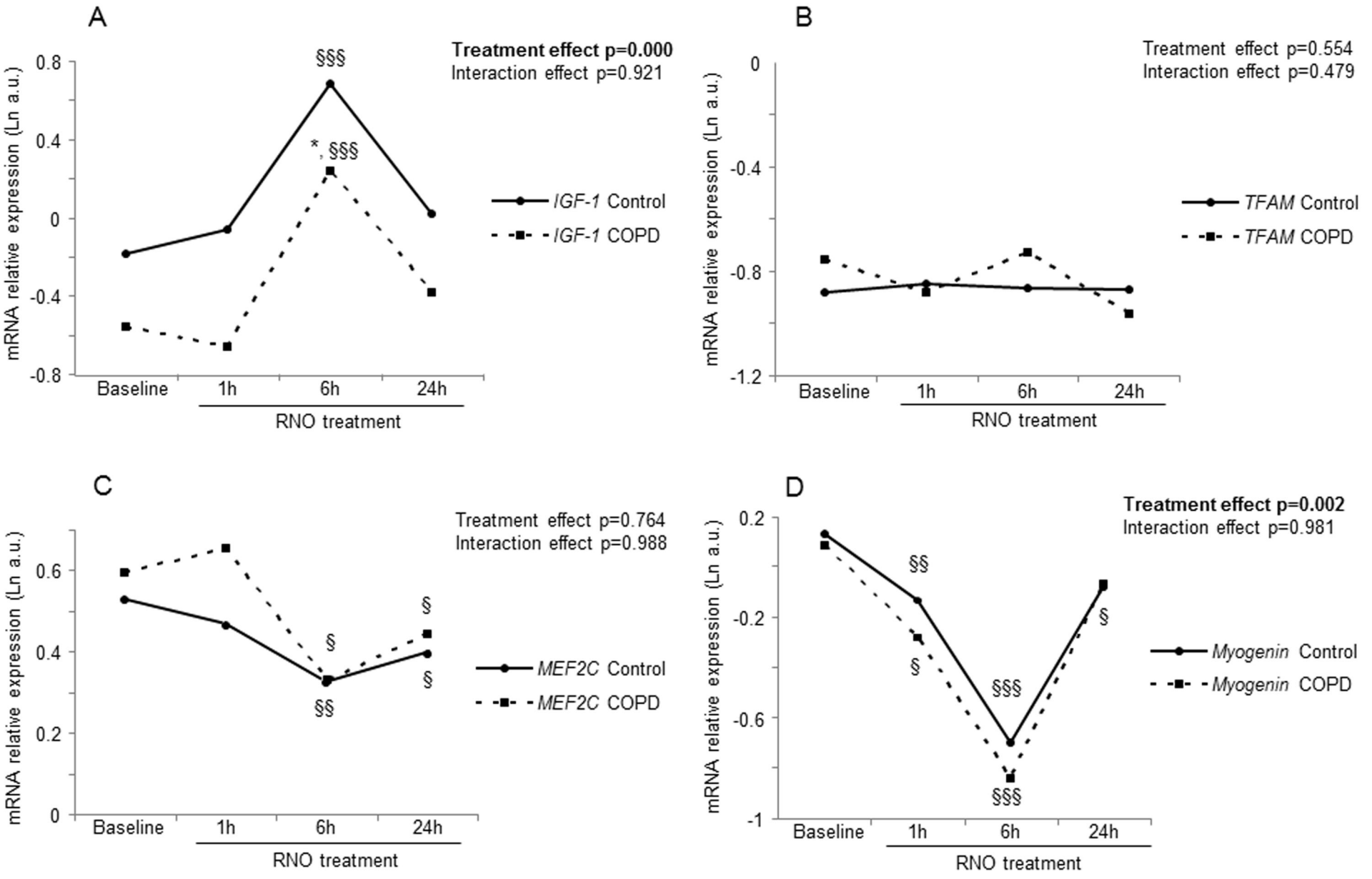

Barreiro E. et al. Figure 6

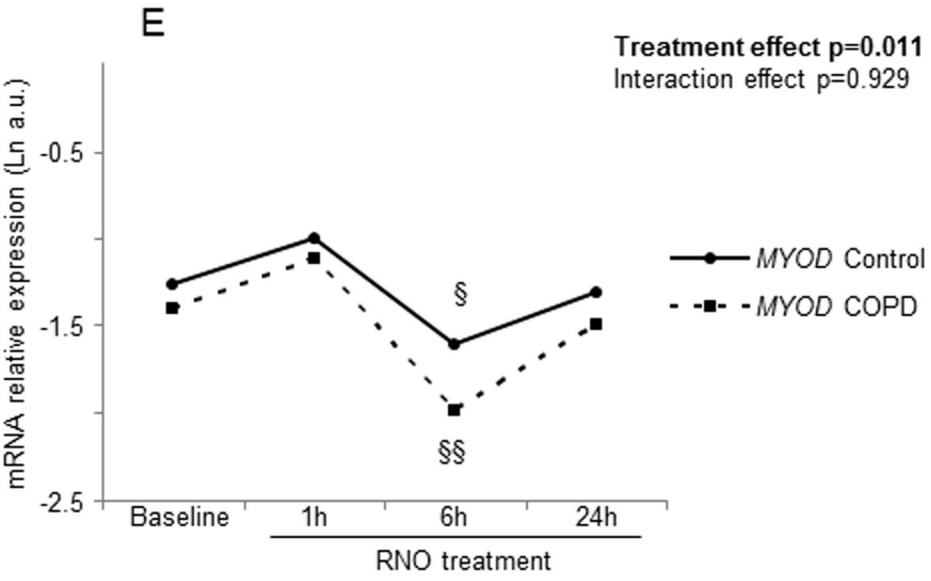

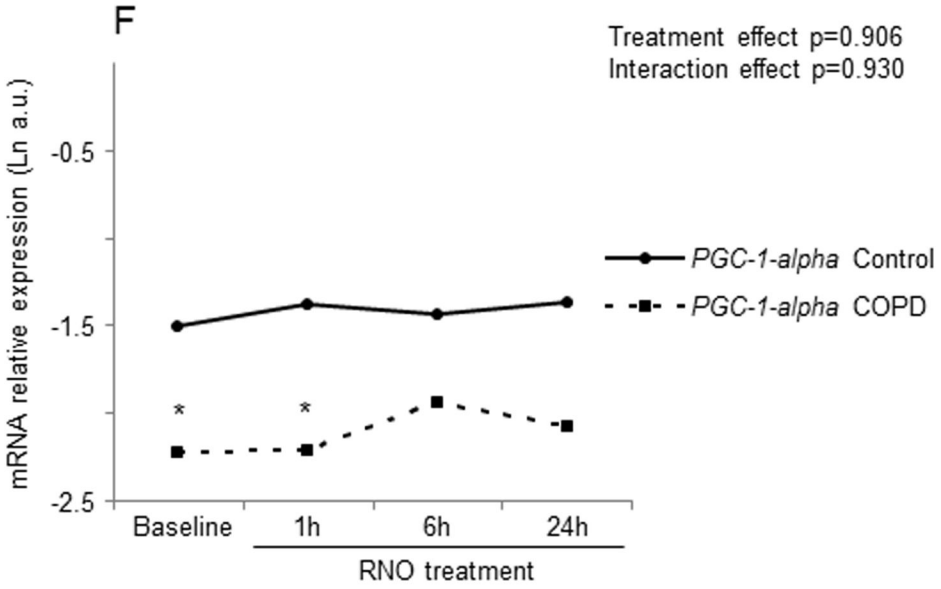

Barreiro E. et al. Figure 7

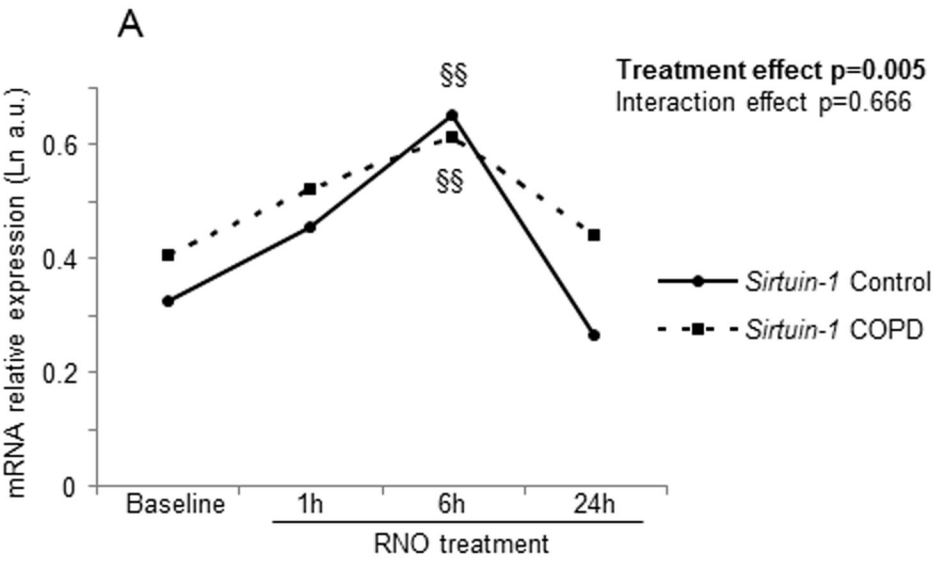

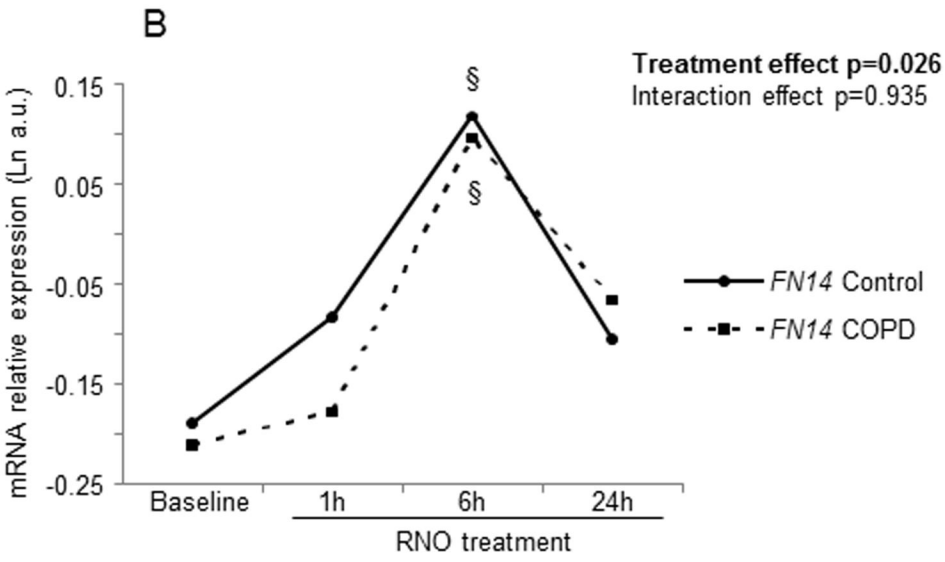

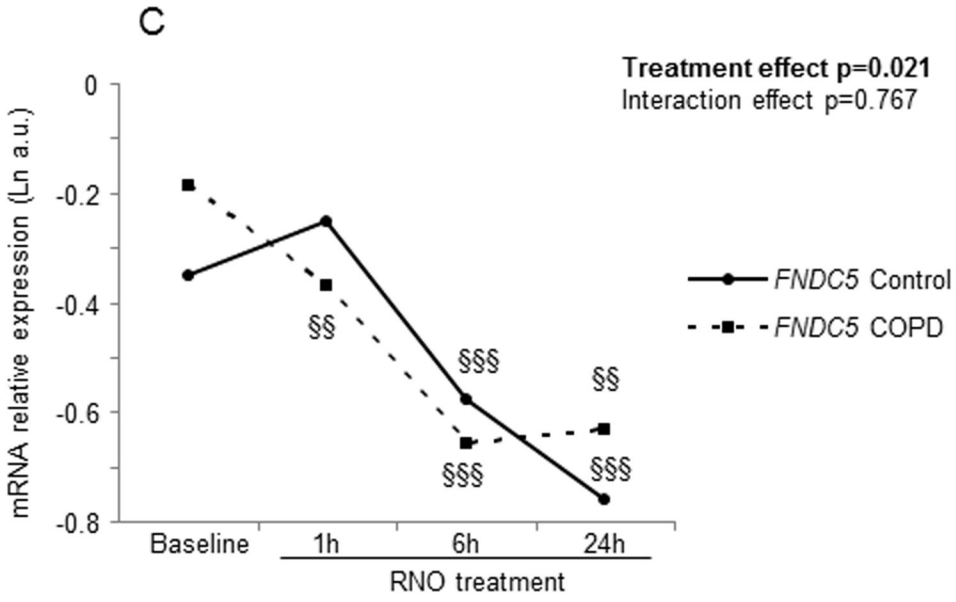

Barreiro E. et al. Figure 8

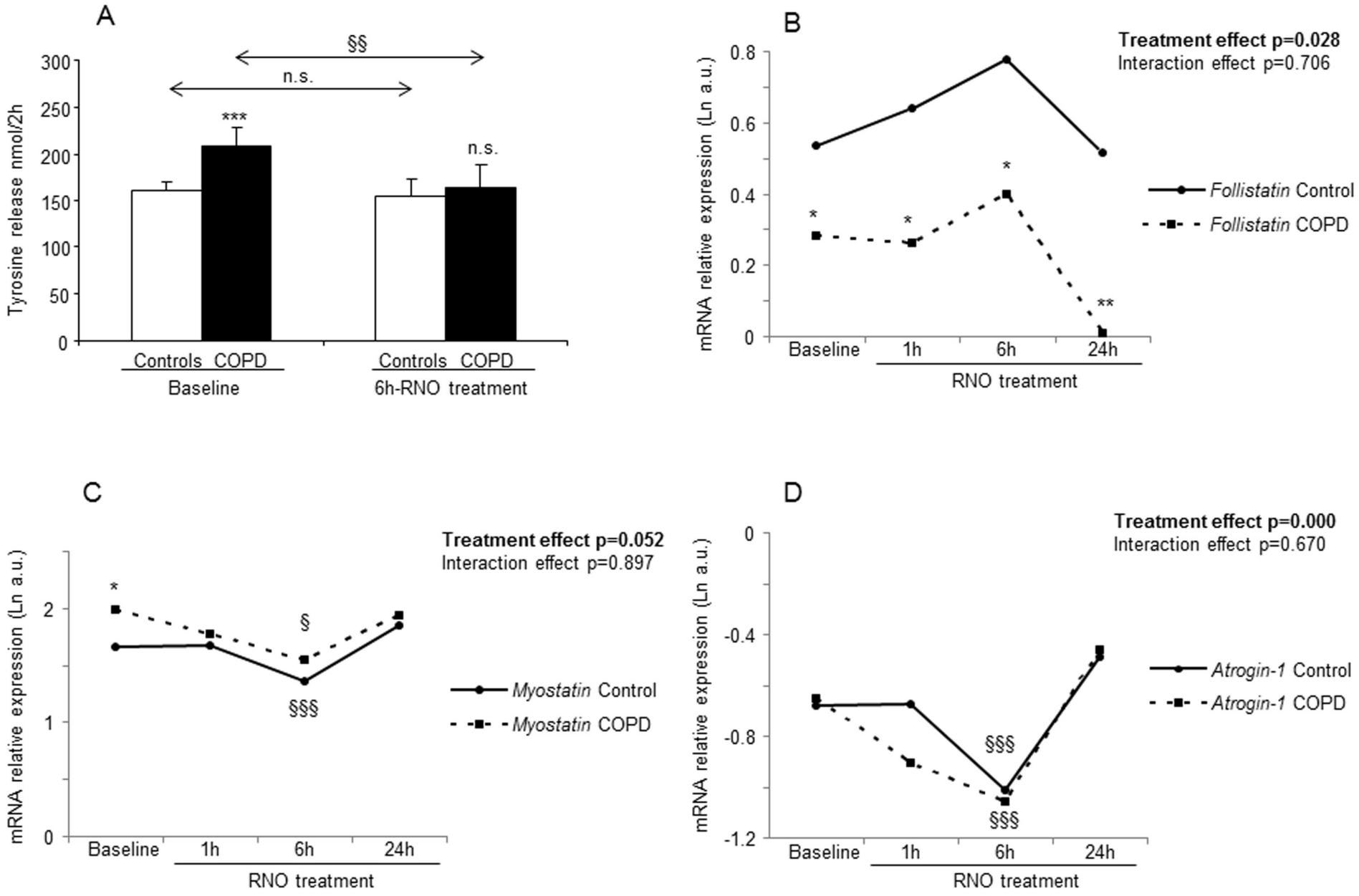

Barreiro E. et al. Figure 8

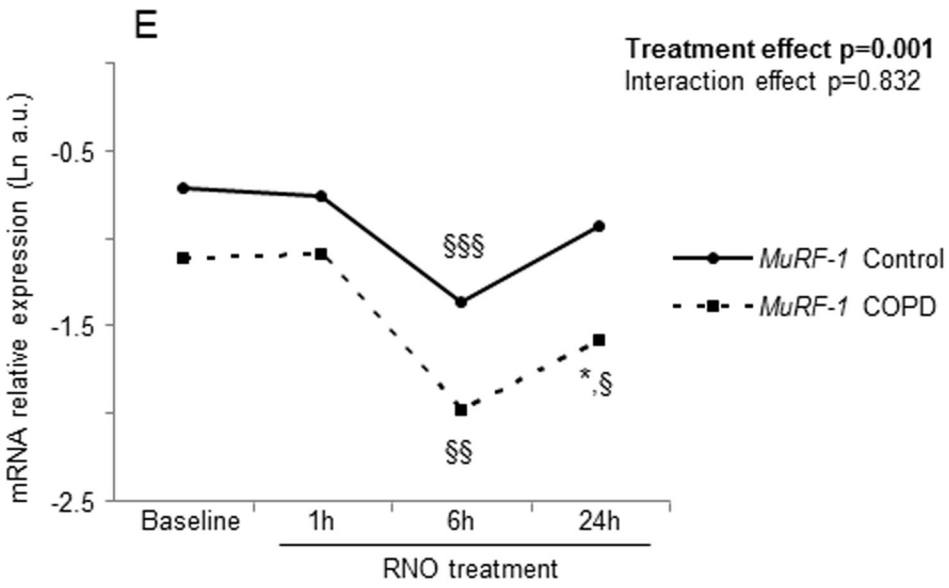

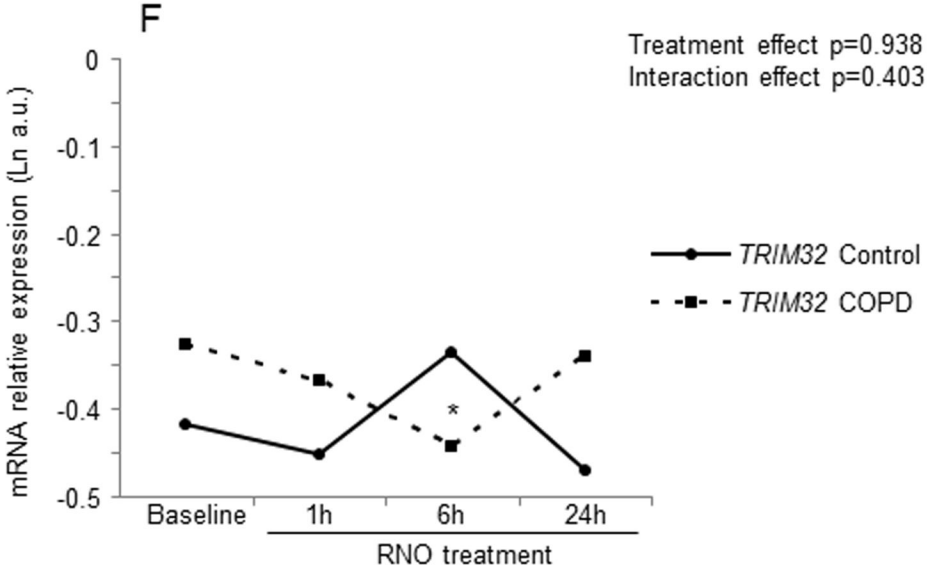

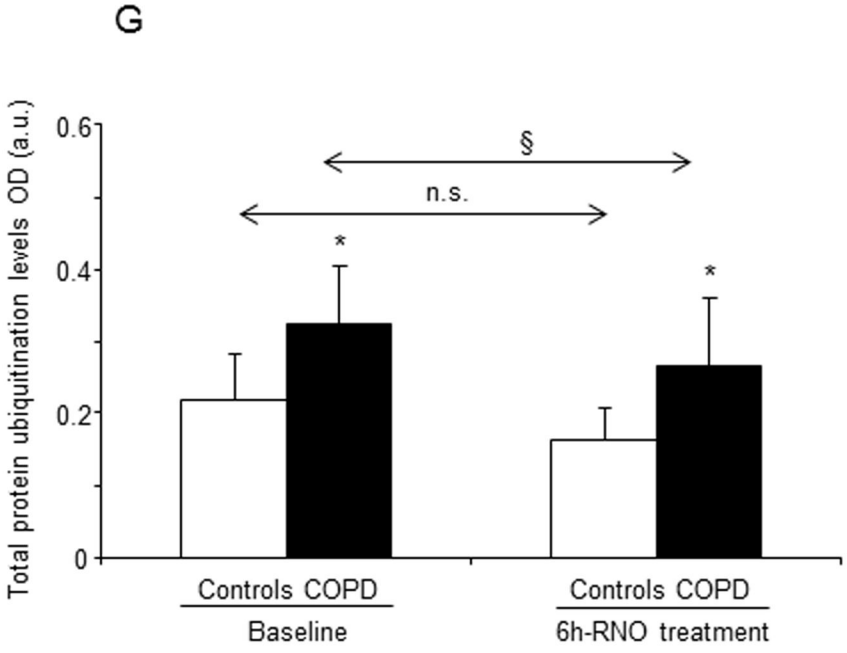

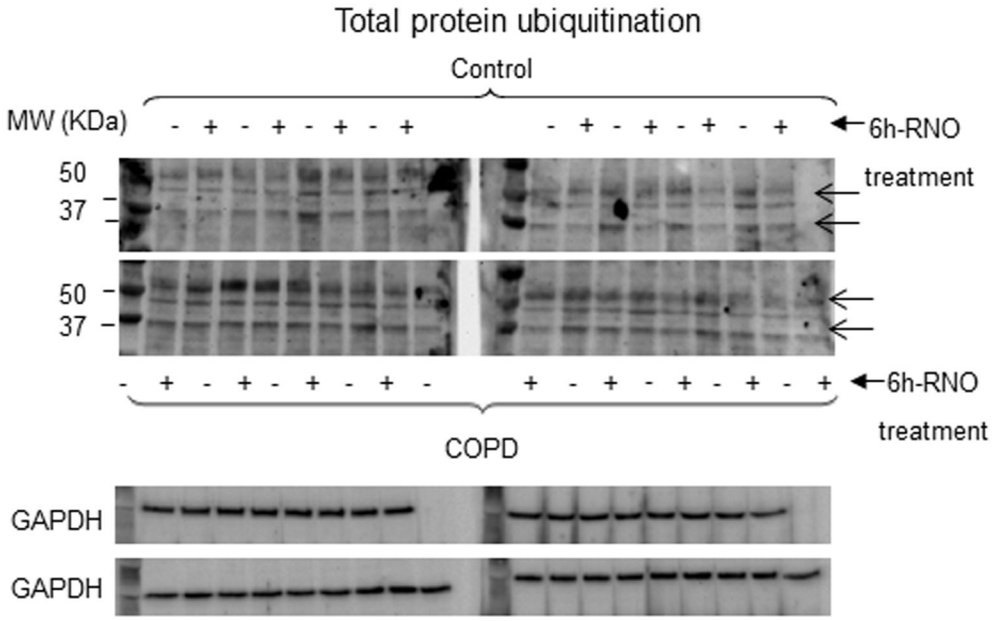

Barreiro E. et al. Figure 9

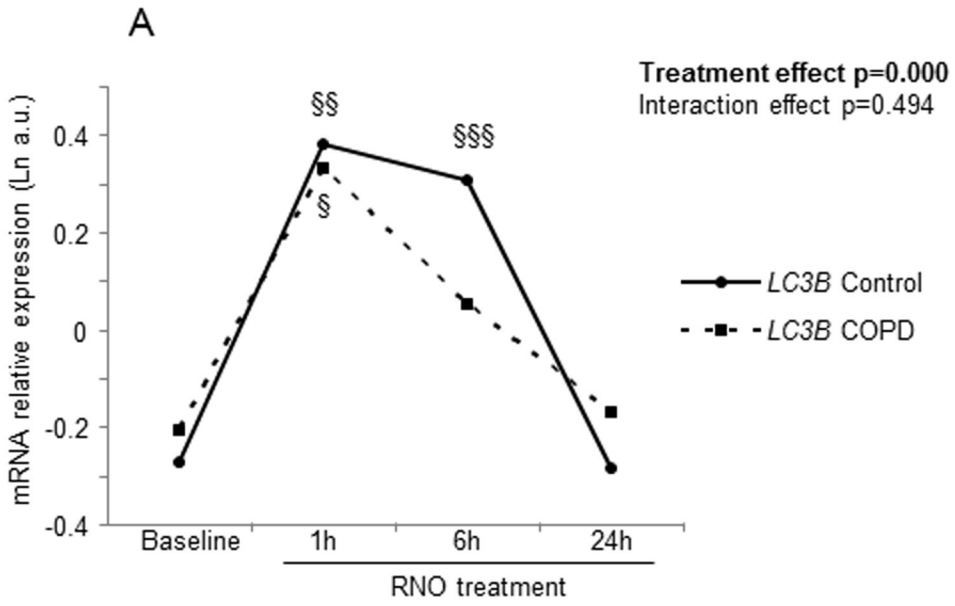

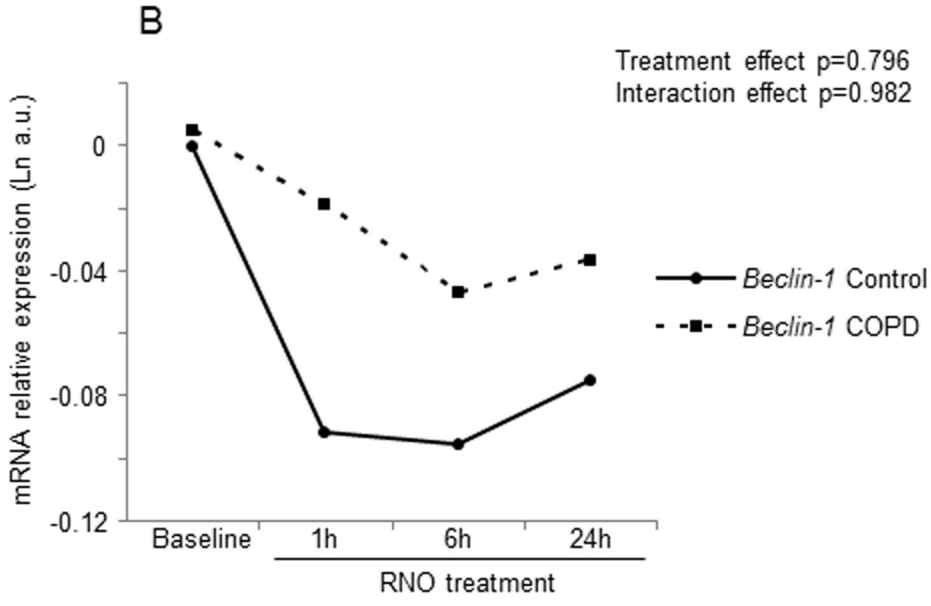

Barreiro E. et al. Figure 10